



## OPEN ACCESS

## EDITED BY

Serge Campeau,  
University of Colorado Boulder, United States

## REVIEWED BY

Chandrashekhara Borkar,  
Tulane University, United States  
Sue Wonnacott,  
University of Bath, United Kingdom  
Arik J. Hone,  
The University of Utah, United States

## \*CORRESPONDENCE

Julie M. Miwa  
✉ jmm312@lehigh.edu

## †PRESENT ADDRESSES

Kristin R. Anderson,  
Departments of Biological and Chemical  
Science, University of Galway, Galway, Ireland  
Peter Rogu,  
New York Institute of Technology College of  
Osteopathic Medicine, Old Westbury, NY,  
United States  
Katie Hoffman,  
Department of Biomedical and Pharmaceutical  
Sciences, University of Montana, Missoula, MT,  
United States  
Krystle J. McLaughlin,  
Department of Chemistry, Vassar College,  
Poughkeepsie, NY, United States  
X. Frank Zhang,  
Department of Biomedical Engineering,  
University of Massachusetts Amherst,  
Amherst, MA, United States

RECEIVED 01 December 2023

ACCEPTED 24 October 2024

PUBLISHED 23 December 2024

## CITATION

Anderson KR, Cao W, Lee HS, Crenshaw MA,  
Palumbo TB, Fisher-Perez E, DeGraaf A,  
Rogu P, Beatty MA, Gracias GM, Pisapati AV,  
Hoffman K, McLaughlin KJ, Hupbach A, Im W,  
Zhang XF and Miwa JM (2024) A novel  
anxiety-associated SNP identified in *LYNX2*  
(*LYPD1*) is associated with decreased protein  
binding to nicotinic acetylcholine receptors.  
*Front. Behav. Neurosci.* 18:1347543.  
doi: 10.3389/fnbeh.2024.1347543

## COPYRIGHT

© 2024 Anderson, Cao, Lee, Crenshaw,  
Palumbo, Fisher-Perez, DeGraaf, Rogu,  
Beatty, Gracias, Pisapati, Hoffman,  
McLaughlin, Hupbach, Im, Zhang and Miwa.  
This is an open-access article distributed  
under the terms of the [Creative Commons  
Attribution License \(CC BY\)](#). The use,  
distribution or reproduction in other forums is  
permitted, provided the original author(s) and  
the copyright owner(s) are credited and that  
the original publication in this journal is cited,  
in accordance with accepted academic  
practice. No use, distribution or reproduction  
is permitted which does not comply with  
these terms.

# A novel anxiety-associated SNP identified in *LYNX2* (*LYPD1*) is associated with decreased protein binding to nicotinic acetylcholine receptors

Kristin R. Anderson<sup>1†</sup>, Wenpeng Cao<sup>2</sup>, Hui Sun Lee<sup>1</sup>,  
Mark A. Crenshaw<sup>1</sup>, Talulla B. Palumbo<sup>1</sup>, Ethan Fisher-Perez<sup>1</sup>,  
Amanda DeGraaf<sup>1</sup>, Peter Rogu<sup>1†</sup>, Maria A. Beatty<sup>1</sup>,  
Gabrielle M. Gracias<sup>1,3</sup>, Avani V. Pisapati<sup>2</sup>, Katie Hoffman<sup>1†</sup>,  
Krystle J. McLaughlin<sup>1†</sup>, Almut Hupbach<sup>4</sup>, Wonpil Im<sup>1,2</sup>,  
X. Frank Zhang<sup>2†</sup> and Julie M. Miwa<sup>1\*</sup>

<sup>1</sup>Department of Biological Sciences, Lehigh University, Bethlehem, PA, United States, <sup>2</sup>Department of Bioengineering, Lehigh University, Bethlehem, PA, United States, <sup>3</sup>BS, Robert Wood Johnson Medical School, Rutgers, The State University of New Jersey, New Brunswick, NJ, United States, <sup>4</sup>Department of Psychology, Lehigh University, Bethlehem, PA, United States

**Introduction:** Anxiety disorders are among the most common mental illnesses in the US. An estimated 31.1% of U.S. adults experience any anxiety disorder at some time in their lives. Understanding some of the molecular underpinnings of anxiety could lead to improved treatments over current strategies focusing on symptom relief rather than root causes. One significant neurotransmitter system exerting control over anxiety is the nicotinic receptor subdivision of the cholinergic system. The murine *Lynx2* gene, encoding a protein modulator of nicotinic acetylcholine receptors, is expressed in anxiety-related neural circuitry in rodents and has been functionally associated with anxiety-like behavior.

**Methods:** We examined variations in the human *LYNX2* (*LYPD1*) gene and their potential effects on anxiety levels in a cohort of 624 participants. Participants completed validated anxiety questionnaires (e.g., STICSA and STAI), which assessed both their current anxiety and their general tendency to experience anxiety. Possible functional alterations due to one such mutation was assessed through atomic force microscopy (AFM) and computational modeling.

**Results:** We identified a previously unreported single nucleotide polymorphism (SNP) in the mature protein-coding region of *LYNX2* that was associated with significantly higher than normal anxiety scores. These elevated scores resembled those seen in patients clinically diagnosed with generalized anxiety disorder and panic disorder, although this genetically defined subpopulation did not typically report such diagnoses. Through computational modeling of the homopentameric  $\alpha 7$  nicotinic receptor subtype and in vitro atomic force microscopy (AFM), we discovered that a specific *LYNX2* SNP is linked to a reduced binding affinity between the *LYNX2* protein and nAChRs, offering a potential functional explanation for the role that this mutation may play in anxiety.

**Discussion:** A polymorphism in *LYNX2*, which codes for an inhibitory modulator of nicotinic acetylcholine receptors, has the potential to lead to sensitized nicotinic receptor activity in anxiety-related circuits. The *LYNX2* protein has been shown to bind to multiple nicotinic acetylcholine receptor subtypes, including  $\alpha 4\beta 2$ ,  $\alpha 7$ , and  $\alpha 3\beta 4$  subtypes, each of which have been shown to be involved

in affective behaviors. This work suggests that a subpopulation of individuals harboring a deleterious mutation in *LYNX2* may predispose them to anxiety through abnormal nicotinic receptor control. In the future, this work may lead to the development of a biomarker for anxiety or a diagnostic tool for the early detection of individuals with susceptibility to anxiety.

#### KEYWORDS

*Lynx2*, *LYPD1*, nicotinic acetylcholine receptors, anxiety disorders, human psychology, human DNA analysis, atomic force microscopy

## 1 Introduction

The stress response is an adaptive set of physiological and psychological changes that induces a response to situations perceived as threatening. If not regulated properly, such responses can manifest into a suite of anxiety, mood, and stress-related disorders. Anxiety disorders are the most prevalent mental disorders in the United States (Bandelow and Michaelis, 2015). Despite this, the exact etiology of such disorders is not fully understood; it likely stems from complex interactions between genetic, psychological, and environmental factors (Feder et al., 2009; Lissek et al., 2014; Duits et al., 2015). Current treatments are therefore largely focused on treating symptoms rather than addressing the biological structures most fundamental to the development of an anxiety disorder (Locke et al., 2015; Williams et al., 2017). This highlights an urgent need to understand the complex underpinnings of anxiety to inform targeted, effective, and accessible treatments.

There has been substantial research uncovering the role of specific genes in the development of anxiety-related disorders (Martin et al., 2009); however, to become clinically useful, more research is needed to determine how specific genetic variants alter the susceptibility or risk of an individual developing an anxiety disorder when combined with environmental stressors (Bystritsky et al., 2013). Additionally, understanding if specific genetic variants increase the risk for developing anxiety disorders can help identify biomarkers, ultimately leading to better diagnostic and preventative measures. Although animal models under controlled exposure have proven useful for uncovering the role of specific genes in various behaviors (Le-Niculescu et al., 2011), biological detection of anxiety disorders remains complex, and examination of the human genome is one way to gain more precise insight into their pathology and treatment.

Studies in animal models have uncovered the role of the *Lynx2* (*Lypd1*) gene in anxiety-related behaviors. *Lynx2* null mutant mice exhibit anxiety-like behavior as measured by light–dark box, elevated plus and social interaction behavioral assays, as well as elevated fear conditioning responses (Tekinay et al., 2009). Murine *Lynx2* is expressed in regions with known involvement in anxiety circuitry, such as the basolateral amygdala, cingulate cortex, and medial prefrontal cortex, as well as in other regions such as the septum, hippocampus, striatum, pedunculo-pontine tegmental nucleus, peripheral neurons, and pontine nuclei (Sherafat et al., 2021; Dessaud et al., 2006; Tekinay et al., 2009) and in human brains, has been shown to be expressed in specialized neurons within the anterior cingulate cortex (Yang et al., 2015). As such, *Lynx2* has neuronal functions outside of anxiety-related behaviors, in addition to processes outside of the nervous system (Wang et al., 2021; Sugimori et al., 2024).

*LYNX2* is a member of the *Ly6/uPAR* gene superfamily, many members of which encode small three-fingered fold receptor-binding proteins (Tsetlin, 2014). Well characterized members within this

superfamily are secreted snake venom proteins such as  $\alpha$ -bungarotoxin, which binds and inhibits nicotinic acetylcholine receptors (nAChRs). The *LYNX2* protein also has been shown to bind to nAChRs but it contains a motif for a GPI-anchor allowing it to embed in the neuronal membrane as a peripheral membrane protein (Pisapati et al., 2021; Paramonov et al., 2020; Zaigraev et al., 2022). nAChRs are ligand-gated ion channels that respond to the natural neurotransmitter acetylcholine, as well as the drug of abuse nicotine, and are implicated in a wide number of processes, including anxiety, but also extend to cognition, addiction, attention to name a few (Mineur et al., 2023). The *LYNX2* protein has been shown to bind to several nAChR subtypes, including  $\alpha 4\beta 2$  (Tekinay et al., 2009),  $\alpha 7$ , and  $\alpha 3\alpha 4$  nAChRs (Pisapati et al., 2021). Some of the biophysical properties of the interaction of *LYNX2* with nAChRs have been studied with  $\alpha 4\beta 2$  nAChRs, the most abundant receptor subtype in the brain. These properties include lower responsiveness to agonist (seen as a rightward shift in  $EC_{50}$ ), faster desensitization of agonist-induced receptor responses (Tekinay et al., 2009), inhibition of calcium fluxes through the receptor, and suppression of surface  $\alpha 4\beta 2$  receptors even upon nicotine exposure (Wu et al., 2015).

Animal studies have demonstrated that nAChRs, including the  $\alpha 7$ ,  $\alpha 3\beta 4$  and  $\alpha 4\beta 2$  subtypes regulate activity in anxiety- and fear-related circuits and have thus been linked to anxiety- and fear-like outputs (Picciotto, 2003; Mineur et al., 2016; Jiang et al., 2016; Wilson and Fadel, 2017; Salas et al., 2003). In humans, individuals report the self-medication of nicotine, an exogenous agonist to nAChRs, for ameliorating anxiety symptoms (Moylan et al., 2012). There is an association between smoking history and mood disorders such as anxiety disorders (Mouro Ferraz Lima et al., 2023) implicating nicotine and nAChRs in anxiety regulation. Further, there is an association between *CHRNA4*, the gene that encodes the  $\alpha 4$  subunit of nAChRs and negative emotionality (Markett et al., 2011). As such, a modulatory protein of nAChRs, such as *LYNX2*, may be a candidate to consider in anxiety regulation in humans (Palumbo and Miwa, 2023; Miwa et al., 2019; Pisapati et al., 2021).

To assess the translational potential of the *LYNX2* (*LYPD1*) gene for affective disorders, we investigated *LYNX2* and its possible association with anxiety in the human population. We chose to analyze the trait and state components of anxiety in this study as both are represented by rodent behavior paradigms that have been shown to be altered in mice lacking *Lynx2* (Tekinay et al., 2009). Trait anxiety is considered an individual's tendency toward anxiety. In mice, it is thought that basal anxiety-like behavior can be assessed in the light–dark paradigm, which is elevated in mice lacking *Lynx2*, and is representative of human trait anxiety (Smelser and Baltes, 2001; O'Leary et al., 2013). In humans, trait anxiety manifests as the kind of persistent anxiety that characterizes Generalized Anxiety Disorder (GAD). State anxiety, on the other hand, is acquired through the

experience of specific external events/stimuli via learned associations, and in mice can be assessed through paradigms such as fear conditioning/extinction (Hascoët et al., 2001; Elwood et al., 2012; O'Leary et al., 2013). State anxiety can manifest as a phobia, which is also a fear response to a specific stimulus. Here, we identified a subpopulation of individuals harboring a protein coding mutation in *LYNX2*, which we find is associated with heightened self-reported levels representative of both state and trait anxiety. We demonstrate in single-molecule binding studies that this mutation causes a change in the interaction strength of the *LYNX2* protein and nAChR complexes.

## 2 Materials and methods

### 2.1 Psychological testing

All tests and the biodemographic/individual information have been approved by the Lehigh University Institutional Review Board. Recruitment was done widely, with the majority of participants being Lehigh University students, but also included students, faculty and administrators at Lehigh and other institutions. All subjects were adults over the age of 18. We collected background information from our participants, which included the following: sex, age, professional/career goals, hobbies/hobby frequency, mental health diagnoses, highest degree attained, medications, smoking habits, alterations related to identity, and previous experience with cognitive/anxiety experiences. This comprehensive data helped us gain insights into the diverse experiences and backgrounds of our participants, allowing us to consider other factors that may contribute to the relevance of our study (Supplementary Table S1). We collected from 624 participants who completed the anxiety questionnaires (STICSA and/or STAI), 179 male participants and 416 female participants, the balance being participants who answered "other" or did not answer that question. The ratio of male and female participants reflected the demographics of the recruitment pool, who were largely Lehigh University natural science students. The average age was 20.7 +/- 0.28 years and ranged from 18 to 63 with a median age of 20. All data underwent a double coding system to ensure anonymity, confidentiality and security of data. Collection of data and samples occurred in batches of roughly 50–100 participants, and samples from each batch were analyzed by different sets of researchers in different locations to reduce the likelihood that a detected SNP allele was a result of a spurious event such as contamination.

The State–Trait Inventory for Cognitive and Somatic Anxiety (STICSA) (Ree et al., 2008) and State–Trait Anxiety Inventory (STAI) (Spielberger et al., 1983) were used to examine human anxiety levels. These tests assess subjects' chronic and current anxiety levels based on self-reports. The STICSA takes cognitive and somatic anxiety dimensions into account. Both tests provide summarized state and trait anxiety scores calculated from frequency ratings that subjects provide for a variety of anxiety-related symptoms. Participants are asked to report on the anxiety symptoms they are experiencing at the time of the test (state) as well as the anxiety symptoms they experience more generally, outside the bounds of the test and throughout their daily lives (trait). The STAI furthermore allows for a standardized interpretation taking into account inherent anxiety level differences in different populations (based on age, student status, etc.). In addition to anxiety tests, a battery of creativity tests which measure convergent and divergent thinking, including the Creativity Behavioral Inventory (CBI), Remote Associates Test (RAT), and Alternative Uses Task

(AUT), were used to examine human creativity due to previous reports of the correlation between creativity and mental illness (Andreasen, 1987; Runco and Richards, 1997; Kyaga et al., 2011; Kyaga et al., 2012). The researchers analyzing the psychology data were different from those performing DNA analysis, to keep the information about SNP carriers blind to those analyzing psychological data.

### 2.2 DNA analysis

Genomic DNA was extracted from saliva samples collected from each participant during psychological testing. Saliva and cheek cells were deposited into conical tubes by the participants after rinsing with a 0.9% saline solution for 60 s. The saline and saliva samples were kept on ice at 4°C for up to one week. A portion of the saliva samples were used for genomic DNA extraction with Chelex resin (BioRad 1421253) following the manufacturer's recommendations within a week of collection. The remainder of the saliva-saline samples were moved into long-term storage at –20° or –80°C. Exons 3–4 of the *LYNX2* gene representing the mature protein coding sequence were amplified with PCR primers (Table 1) 100–200 bp outside of the exon/intron boundaries. Primers were identified by comparing isoform cDNA sequences from NCBI (GeneBank name: *LYPD1*, chromosomal location 2q21.2). Successful PCR reactions were purified using ExoSap (Affymetrix cat no.: 78200) or by gel excision of visualized bands and gel extraction (GeneJET Gel Extraction Kit, ThermoFisher, K0691). Purified PCR products were sent to GenScript USA for Sanger sequencing. Chromatogram analyses of sequence files were performed using DNA Baser Sequence Assembler software to generate contigs of overlapping sequences under the high-quality option. If a contig did not form under high quality, the results were discarded, and PCR was performed again for high-quality sequence results.

Alternative allele detection was conducted using manual identification of the chromatograms by more than one individual to verify alternative allele identification. Alignment to the reference genome (GRCh38) was done using Molecular Evolutionary Genetics Analysis (MEGA) software. We performed 2x sequence coverage on all samples using both a forward and reverse sequencing primer, analyzing in large batches of samples, with further in-depth (4–6x) sequence coverage for select samples. Samples from individuals with variant alleles and a representative number of reference samples were further confirmed through extra rounds of amplification and sequencing, as well as re-extraction of DNA, each performed by unique researchers. Eight of the nine identified SNPs were in dbSNP.<sup>1</sup> The ninth SNP was not previously reported in dbSNP, Gnomad<sup>2</sup>, or Bravo<sup>3</sup> at the time of publication.

### 2.3 Computational modeling and simulation of *LYNX2*/α7 nAChR complexes

The structure of two adjacent α7 subunits (α7:α7) was taken from the Protein Data Bank (PDB) entry 3SQ6 (Li et al., 2011). The α7 subunits have a closed state conformation of loop C. We obtained 350

1 <https://www.ncbi.nlm.nih.gov/snp/>

2 <https://gnomad.broadinstitute.org/>

3 <https://bravo.sph.umich.edu/freeze8/hg38/>

TABLE 1 PCR Primers used for targeted sequencing of *LYNX2*.

	Exon 2 (ENSE00003691134)	Exon 3 (ENSE00001384648)
Forward	5'-GTGGGATGGTCGTGATTCCG-3'	5'-GGGACAGCTATTCTTTTGCC-3'
Reverse	5'-CGATAAATTACCGGGGAGTG-3'	5'-CTCCTTGCTCACCACCAC-3'

$\alpha 7:\alpha 7$  snapshots with apo-state loop C conformations from a 10 ns molecular dynamics (MD) simulation by applying a weak positional restraint to glutamate185 C $\alpha$  atom in the loop C.

The three-dimensional (3D) structure of *LYNX2* was predicted from the sequence using the standalone I-TASSER suite (Yang et al., 2015) by specifying a *LYNX1* PDB structure (PDB entry 2 L03) (Lyukmanova et al., 2011) as a template. We obtained 100 energy-minimized snapshots from a 5 ns MD simulation of the *LYNX2* model and then identified the best snapshot among them by evaluating the quality of each structure using ModFOLD (Maghrabi and McGuffin, 2017). For the best snapshot, we sampled thermally acceptable 50 conformations for *LYNX2* loop I using the Backrub application in Rosetta (Smith and Kortemme, 2008).

A low-resolution structure model of  $\alpha 7$  nAChR in complex with *LYNX2* was generated based on our *LYNX1*/ $\alpha 4:\alpha 4$  complex model (Nissen et al., 2018). The  $\alpha 7$  subtype was chosen because a homomeric subtype was more tractable to model than heteromeric nAChRs  $\alpha 4\beta 2$  and  $\alpha 4\beta 2$  subtypes, to which *LYNX2* also binds. A set of *LYNX2*/ $\alpha 7:\alpha 7$  complex models was built by mapping each  $\alpha 7$  subunit (in the ensemble of 350  $\alpha 7:\alpha 7$  conformations) and each *LYNX2* (in the ensemble of 50 *LYNX2* conformations) onto  $\alpha 4:\alpha 4$  and *LYNX1* in the *LYNX1*/ $\alpha 4:\alpha 4$  model, respectively, thus generating  $350 \times 50$  combinations. For each complex, *LYNX2* was moved outwards from  $\alpha 7:\alpha 7$  by  $\leq 2$  Å using an interval of 1 Å along a vector defining the geometric centers of two protein binding surfaces to find a complex structure with the minimum number of bad (energetically unfavorable) contacts between  $\alpha 7:\alpha 7$  and *LYNX2*, which was determined as the final model of  $\alpha 7$  nAChR in complex with *LYNX2* (Supplementary Figure S1).

The *LYNX2*/ $\alpha 7:\alpha 7$  complex model was subjected to 135 ns MD simulations to obtain a refined complex model. 5 ns simulations with or without weak positional restraints were iterated during the first 35 ns simulations. The positional restraint was applied to the Q39 C $\alpha$  atoms of *LYNX2*, aiming at maintaining *LYNX2* loop II in the ligand-binding pocket under  $\alpha 7:\alpha 7$  loop C by gradually reducing the force constant. We also applied positional restraints to prevent  $\alpha 7:\alpha 7$  from dissociating; no restraints were applied to loop B, loop C and  $\beta 8$ – $\beta 9$  loop in  $\alpha 7:\alpha 7$ , allowing for conformational flexibility, as they involve protein–protein interactions. After the 35 ns simulation, we removed the positional restraints to *LYNX2* and performed additional 100 ns simulations for equilibration.

The Q61H mutation of the full-length *LYNX2* gene (the nascent polypeptide before cleavage of the signal sequence) is at amino acid 39 in the fully-processed mature *LYNX2* protein and will be referred to as Q39H. To generate the *LYNX2* Q39H alternative allele, we computationally replaced *LYNX2* Q39 with histidine in the  $\alpha 7:\alpha 7$ /*LYNX2* complex structure refined by MD simulations (Supplementary Figure S1). We carried out 400 ns MD simulation without any positional restraints to *LYNX2* for three independent replicates (MD-1, MD-2, and MD-3) of  $\alpha 7:\alpha 7$  in complex with native *LYNX2* and its Q39H alternative allele. The convergence of the simulations was assessed by measuring root-mean-square deviation (RMSD) of *LYNX2* in terms of simulation time, indicating that MD-3 s of each system show good convergence (Supplementary Figure S1C).

The trajectories of these well-converged replicates were then analyzed to calculate nonbonded interaction (van der Waals and electrostatic) potential energies between the entire  $\alpha 7:\alpha 7$  interface and *LYNX2*. Note that, to calculate the RMSD, we first aligned  $\alpha 7:\alpha 7$  of each MD snapshot to the initial structure (i.e., the structure before the MD simulations) and then calculated the RMSD of the entire *LYNX2* C $\alpha$  atoms relative to its initial structure. Therefore, the calculated RMSD includes both the *LYNX2* conformational changes and the changes of *LYNX2* positions relative to  $\alpha 7:\alpha 7$ . Given the flexibility of  $\alpha 7:\alpha 7$ /*LYNX2* interactions, RMSD values above 5 Å appear to be reasonable and  $\alpha 7:\alpha 7$  and *LYNX2* interact strongly as shown in Supplementary Figure S1C (the interaction energy time series) (Dong et al., 2020).

All MD simulations were prepared through CHARMM-GUI (Jo et al., 2008; Lee et al., 2016) and performed with explicit water molecules and 150 mM NaCl using CHARMM36m force field (Huang et al., 2017) and NAMD software (Phillips et al., 2005) at 300 K.

## 2.4 Proteins

Recombinant hexahistidine-tagged human *LYNX2* gene was made in the pcDNA3.1 plasmid, expressed in HEK 293 T cells and purified from culture supernatant using Ni-NTA chromatography. The expression and purification of the protein were confirmed by SDS-PAGE and Western blot using an anti-his-HRP antibody.

## 2.5 Protein immobilization

Purified recombinant *LYNX2* was attached to an atomic force microscopy (AFM) cantilever by covalently cross-linking the two using a heterobifunctional PEG linker (Ebner et al., 2007). The AFM cantilevers (MLCT: Bruker Nano, Camarillo, CA) were first silanized with 3-aminopropyltriethoxysilane (APTES) using a gas phase coating method (Wildling et al., 2011). An acetal-PEG27-NHS linker was then attached to the silanized cantilevers in chloroform via its N-Hydroxysuccinimide (NHS) group and then rinsed and dried under nitrogen gas. Next, the acetal group of the PEG linker was converted to an aldehyde group using a 1% citric acid solution vol/vol, and 1  $\mu$ M of *LYNX2* was then added to the solution, which coupled to the activated PEG linker. After quenching the free aldehyde group with ethanolamine, the cantilevers were stored in TBS buffer (50 mM Tris, 0.15 M NaCl, pH 7.4) until experimental use.

## 2.6 AFM apparatus

All single-molecule force measurements were conducted using a custom-designed AFM that employs a single-axis piezoelectric translator equipped with a strain gauge (Physik Instrumente, Waldbronn, Germany) to control the absolute position of the AFM cantilever (Chen and Moy, 2002; Zhang et al., 2002; Zhang et al., 2004; Fu et al., 2015). The deflection of the cantilever was monitored

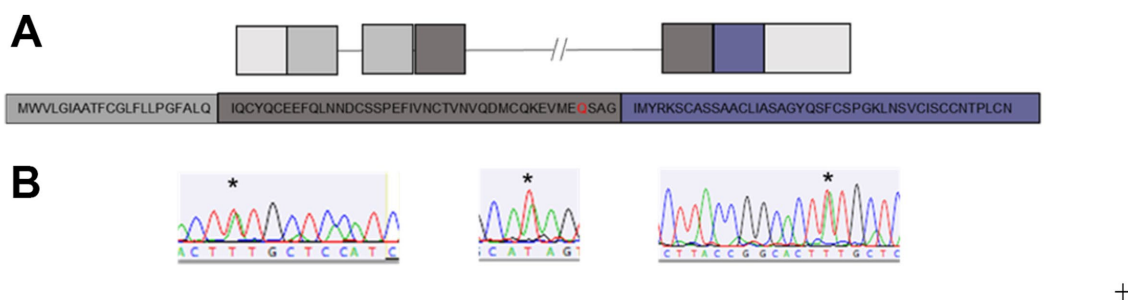


FIGURE 1

Wild-type Human *LYNX2* gene mutants. **(A)** Schematic of the wild-type human *LYNX2* gene and corresponding amino acid sequence. Light grey = UTR, dark grey = signal sequence, black = exon 3, blue = exon 4. **(B)** Representative chromatographs from mutant individuals, stars show heterozygous peak.

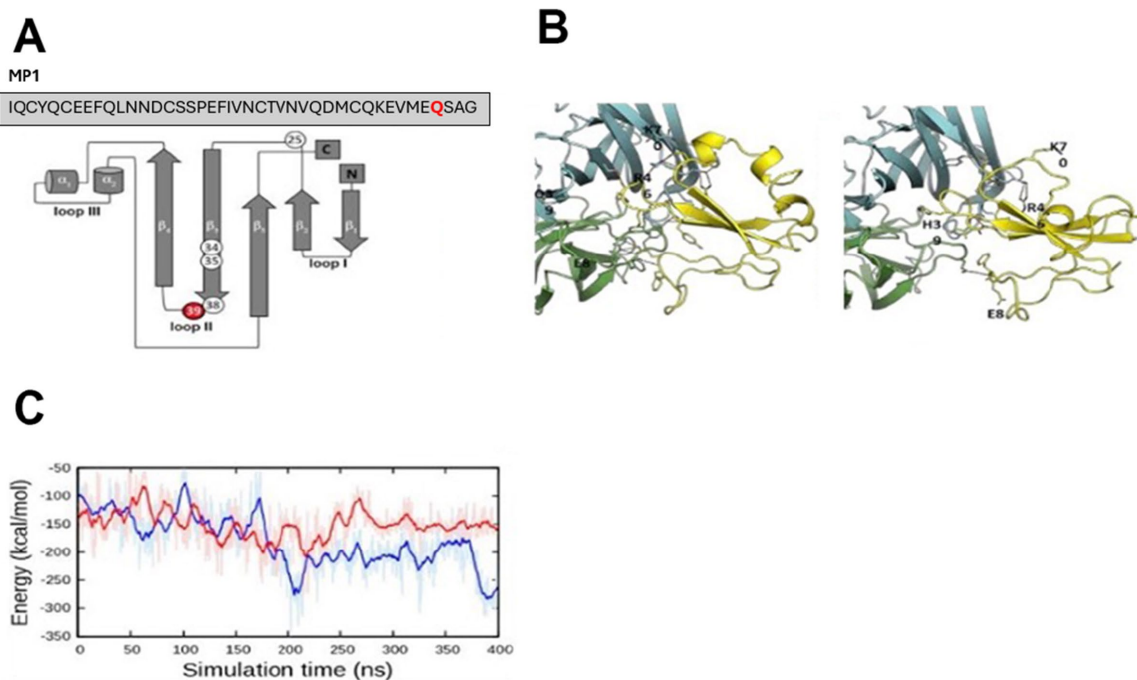


FIGURE 2

Protein modeling of *LYNX2* and *LYNX2*/ $\alpha 7$  nAChR interaction. **(A)** Human *LYNX2* protein structure schematic. **(B)** Left: Structural details of  $\alpha 7$ : $\alpha 7$  in complex with native *LYNX2*. The last 400-ns simulation snapshot was used for this structural illustration. Two  $\alpha 7$  subunits are in green and cyan. *LYNX2* is colored yellow. Hydrogen bonds between  $\alpha 7$ : $\alpha 7$  and *LYNX2* are highlighted using orange dotted lines. Right: Structural details of  $\alpha 7$ : $\alpha 7$  in complex with mutant *LYNX2*. The last 400 ns simulation snapshot was used for this structural illustration. Two  $\alpha 7$  subunits are in green and cyan. *LYNX2* is colored yellow. Hydrogen bonds between  $\alpha 7$ : $\alpha 7$  and *LYNX2* are highlighted using orange dotted lines. **(C)** Interaction energy between  $\alpha 7$ : $\alpha 7$  and *LYNX2* during the simulations.

optically using an inverted optical system attached to the AFM. A focused laser spot from a fiber-coupled diode laser was reflected off the back of the cantilever onto a two-segment photodiode to monitor the cantilever deflection. The photodiode signal was then pre-amplified, digitized and processed by a computer. The force apparatus was suspended inside a refrigerator housing to reduce both mechanical and thermal instabilities.

The human  $\alpha 7$  nAChR receptor was expressed on SH-EP1 cells by transfection of pCEP4 vector containing the cDNA of the  $\alpha 7$  receptor. The stably transfected SH-EP1- $\alpha 7$ -nAChR cell line was previously engineered and characterized as described in Zhao et al. (2003). The transfected cells were maintained in media supplemented with

0.13 mg/mL hygromycin B. The cells were plated on 35 mm cell culture dish 24 h prior to AFM force measurements.

## 2.7 AFM force measurements of individual *LYNX2*/ $\alpha 7$ nAChR interactions

The AFM force measurements were performed on an apparatus designed for operation in the force spectroscopy mode (Zhang et al., 2002; Zhang et al., 2004; Zhang et al., 2009; Fu et al., 2015). Using a piezoelectric translator, the *LYNX2*-functionalized cantilever tip was lowered onto a live SH-EP cell expressing  $\alpha 7$  nAChRs (Figure 2A).

Tip-cell contact may (or may not) lead to LYNX2/ $\alpha$ 7 nAChR interactions. The binding interaction was then determined from the deflection of the cantilever via a position-sensitive two-segment photodiode. To calibrate the cantilever (320  $\mu$ m long by 22  $\mu$ m wide triangle), the spring constant at the tip was characterized via thermally induced fluctuations (Hutter and Bechhoefer, 1993). The spring constants ( $9.7 \pm 1.9$  pN/nm) of the calibrated cantilevers agreed with the values specified by the manufacturer.

Except for the adhesion specificity test (Supplementary Figure S1D), the contact time and indentation force between the cantilever and the sample were minimized to obtain measurements of the unitary unbinding force. An adhesion frequency of  $\sim 30\%$  in the force measurements ensured that there was a  $> 83\%$  probability that the adhesion event was mediated by a single LYNX2/ $\alpha$ 7 nAChR bond (Evans, 2001). AFM measurements were collected at cantilever retraction speeds ranging from 0.1 to 10  $\mu$ m/s in order to achieve the desired loading rate ( $\sim 30$ – $4,000$  pN/s). All measurements were conducted at  $25^\circ\text{C}$  in the cell culture medium. Loading rates were determined directly from the force-extension data by multiplying the system spring constant (Figure 2A) of the unbinding pulling trace by and the retraction speed of the cantilever.

## 2.8 Dynamic force spectroscopy

The Bell-Evans model, a theory to determine energy landscape properties, describes the influence of an external force on the rate of bond dissociation (Bell, 1978; Evans and Ritchie, 1997). According to this model, a pulling force,  $f$ , distorts the intermolecular potential of a receptor-ligand complex, leading to a lower activation energy and an increase in the dissociation rate  $k(f)$  or a decrease in the lifetime  $t(f)$  as follows:

$$k(f) = \frac{1}{t(f)} = k^0 e^{\left(\frac{f\gamma}{k_B T}\right)} \quad (1)$$

where  $k^0$  is the dissociation rate constant in the absence of a pulling force,  $\gamma$  is the width of the activation barrier, or the position along the reaction coordinate relative to the bound state,  $T$  is the absolute temperature, and  $k_B$  is the Boltzmann constant. For a constant loading rate  $r_f$ , the probability density for the unbinding of the complex as a function of the pulling force  $f$  is given by:

$$P(f) = k^0 e^{\left(\frac{\gamma f}{k_B T}\right)} e^{\left\{ \frac{k^0 k_B T}{\gamma r_f} \left[ 1 - e^{\left(\frac{f\gamma}{k_B T}\right)} \right] \right\}} \quad (2)$$

with the most probable unbinding force  $f^*$ .

$$f^* = \frac{k_B T}{\gamma} \ln\left(\frac{\gamma}{k^0 k_B T}\right) + \frac{k_B T}{\gamma} \ln(r_f) \quad (3)$$

Hence, the Bell-Evans model predicts that the most probable unbinding force  $f^*$  is a linear function of the logarithm of the loading rate. Experimentally,  $f^*$  was determined from the mode of the unbinding force histograms. The Bell-Evans model parameters were determined by fitting Equation 3 to the plot of  $f^*$  versus  $\ln(r_f)$ .

## 2.9 Statistical analysis (methods)

The STAI (State-Trait Anxiety Inventory) was administered in this study because it distinguishes clearly between “state” anxiety, which refers to anxiety being experienced at the time of assessment, and “trait” anxiety, which predicts the degree to which a person is prone to generalized anxiety. To assess participants’ ( $n = 624$ ) state and trait anxieties, the complete STAI test was administered to two cohorts, which we will refer to as the “discovery cohort” and the “replication cohort.”

Half of the STAI addresses state anxiety, and participants are asked to answer assessment items intuitively and in accordance with their present feelings. This part of the test includes items such as “I feel calm,” “I am tense,” and “I feel satisfied,” and participants are asked to characterize their agreement with the statement on a scale of 1–4. 1 corresponds to the answer “Not at all,” and 4 to the answer “Very much so.”

The other half addresses trait anxiety, in which participants are asked to answer in accordance with their feelings in general, and beyond the scope of the time in which the test was taken and into their daily lives. This part of the test includes items such as “I feel pleasant,” “I feel satisfied with myself,” and “I lack self-confidence,” and participants are asked to characterize their agreement with the statement on the same scale of 1–4.

To score the STAI, we added the scoring weights of each question in accordance with the official manual. For the statements which indicate more anxiety (e.g., “I feel tense”), a participant scoring of 4 corresponds to an item weight of 4, and a participant scoring of 1 corresponds to an item weight of 1. For the statements that, inversely, indicate less anxiety (e.g., “I feel calm”), a participant scoring of 4 corresponds to an item weight of 1, and a participant scoring of 1 indicates an item weight of 4, such that the increased weight of an item corresponds to more anxiety-expressing responses.

The scoring of the STICSA was comparable to that of the STAI. The STICSA also makes the distinction between state and trait anxieties, and total scores were calculated by the summation of the items’ weights, in accordance with the STICSA manual. STAI responses were analyzed according to the STAI manual.

Statistical analysis involved comparing scores of human LYNX2 mutant populations to scores of the LYNX2 WT, or reference, population. This was done with a two-tailed Fisher’s Exact Test, or an independent two-tailed  $t$ -test, to determine whether there existed a statistically significant difference between the means of the groups. In some tests, we combined state and trait results of the STICSA and STAI to produce a “total score,” and in others, we made the distinction between state and trait in order to test them separately. In performing a Fisher’s Exact Test to compare scores between human participants with and without the LYNX2 Q39H mutation, we chose a threshold score of 43 for the STICSA test based on literature determining that it was the score that could predict incidence of an anxiety disorder in individuals (Van Dam et al., 2013). For the STAI, we chose a threshold score of 45 as a score that has been used in literature to represent “high anxiety” (Kayikcioglu et al., 2017).

The Creative Behavioral Inventory, CBI, was analyzed with a Fisher Exact Test comparing the average total CBI score of those with the Q39H mutation and the reference group. The CBI total score is determined by summing the individual scores of its components, which are Literature, Music, Crafts, Art, Math & Science, and Performing Arts. Average scores for mutant and reference groups were found and compared, according to each population’s size.

## 2.10 AFM

For each pulling speed, over 1,000 force curves were recorded, which yielded 80 to 350 unbinding forces. Curve fitting was performed using IGOR Pro or Origin software by minimizing the chi-square statistic for the optimal fit. Unless otherwise stated, the data is reported as the mean and the standard error of the estimate. Statistical analyses between groups were performed using an unpaired *t*-test or ANOVA, with a *p*-value less than 0.05 considered to be statistically significant.

## 3 Results

### 3.1 *LYNX2* variants are associated with altered anxiety phenotypes

To assess if *LYNX2* has an impact on human anxiety, we investigated whether there is a correlation between variation in the *LYNX2* gene and self-reported anxiety in a population of 624 participants. The average age of our available population ( $M = 20 \pm 0.28$  years) was below the average age of clinical diagnosis of anxiety disorders at the time of testing ( $M = 30$ , Gonçalves and Byrne, 2012; Vaingankar et al., 2013; Lijster et al., 2017). We used two established tests of self-reported anxiety for phenotyping: the State-Trait Inventory for Cognitive and Somatic Anxiety (STICSA) and the State-Trait Anxiety Inventory (STAI). The STICSA was chosen because it is designed to discriminate between symptoms of anxiety and depression. These two disorders are often comorbid, which can make interpretation of genetic risk for anxiety difficult. The STAI was chosen because it can discriminate between the state and trait components of anxiety (Oei et al., 1990; Grös et al., 2007; Elwood et al., 2012; Van Dam et al., 2013).

After extracting DNA and performing targeted Sanger sequencing, we detected SNPs in nine different positions across the mature protein coding sequence of *LYNX2* (Figure 3A). Eight of the nine SNPs were previously reported in dbSNP, and consisted of a mix of synonymous, missense, and frameshift mutations (Table 2). We did not find enough participants harboring these eight mutations to draw conclusive results about how they function in anxiety. One SNP, however, was not previously reported: (Tables 2, 3) a C → T missense variant resulting in a glutamine (Q) to histidine (H) substitution at amino acid 61 of the full-length protein, and amino acid 39 of the mature protein. We will refer to this variant as Q39H. This was the most common SNP variant in our population, occurring in 14/624 (2.2%) of participants, and was exclusively heterozygous. The Q39H variant was found across different batches of samples throughout the course of the study (Supplementary Table S1). None of the nine variants had been previously associated with anxiety or had pre-existing reports of clinical significance.

As a group, individuals harboring any alternative SNP allele in *LYNX2* reported significantly higher STICSA and STAI scores than those with a reference allele ( $p = 0.005$ ; Cohen's  $d = 1.34$ , Table 3) (Figure 1B). The individuals with the Q39H mutation, in particular, were associated with significantly increased anxiety scores comparable to those clinically diagnosed with an anxiety disorder. Including anxiety, panic attacks, and PTSD. In the STICSA test (Figure 3), the Q39H group was significantly different from the reference group in all measured anxiety tests, with a general value (representative of trait

anxiety) of  $48.43 \pm 2.11$ , and the reference group  $36.60 \pm 0.40$  ( $p < 1.0 \times 10^{-4}$ ), and “at the moment” value of  $45.86 \pm 2.50$  compared to the reference group of  $33.92 \pm 0.40$  ( $p < 1.0 \times 10^{-4}$ ). In the STAI test, the Q39H group was also significantly different from the reference group, with a “general” value (representative of trait anxiety) of  $54.07 \pm 2.79$ , and the reference group  $43.28 \pm 0.49$  ( $p = 4.0 \times 10^{-4}$ ), and “at the moment” value (representative of state anxiety) of  $46.93 \pm 2.79$  compared to the reference group of  $37.94 \pm 0.49$  ( $p = 0.0281$ ) (Table 2; Figure 3). We found two individuals harboring a synonymous mutation at the same location (nucleotides encoding amino acid 39 of the mature protein and amino acid 61 of full length *LYNX2*) with anxiety levels similar to the reference group. This suggests that only the nonsynonymous mutations confer a functional consequence.

We further analyzed the anxiety test results by comparing answers from questions that matched the Diagnostic and Statistical Manual of Mental Disorders (DSM-5) criteria for Generalized Anxiety Disorder (GAD), an anxiety disorder reflective of increased trait anxiety (Chambers et al., 2004). We identified 11 questions that matched diagnosis symptoms. In these DSM-aligned questions, the Q39H group answers reflected significantly higher anxiety scores (Figure 3D). These data suggest a relationship between the *LYNX2* mutation Q39H and heightened anxiety levels. The individuals with the Q39H mutation in *LYNX2* also had anxiety scores comparable to those of individuals with diagnosed panic disorder (Van Dam et al., 2013). 61.5% of individuals harboring the Q39H had high anxiety levels, above the levels for GAD, whereas in the reference group, 15.9% of respondents exhibited such levels. There was good concordance in the entire dataset between the STICSA and STAI values including the reference group and the Q39H carriers (Figure 4). This suggests a functional consequence of the mutation in elevating anxiety levels, indicating its potential role in predisposing individuals to heightened anxiety traits.

To explore a previously discovered link between creativity and heightened trait anxiety levels, we performed and analyzed the results of the Creative Behavioral Inventory (CBI), taking interest in the comparison of scores between those harboring the Q39H mutation and those not (Figure 5). We found there to be a significant difference between the average scores of the groups, with a Q39H group score of  $30.35 \pm 4.79$  and a reference group score of  $43.46 \pm 1.62$  ( $p = 0.45$ ). This provides evidence for a link between the Q39H mutation and creativity.

### 3.2 Mutated human *LYNX2* protein binds with less affinity to $\alpha 7$ nAChRs

To study the possible effect of the most common Q39H variant on nAChR binding, we performed computational modeling and binding studies with the human *LYNX2* protein and a nAChR subtype. The Q39H mutation is at amino acid 39 in the mature protein (Figure 2A). In the mature protein the 39th amino acid mutation site is at the tip of loop II (Figure 2A), a region associated with nAChR binding similar to three-looped nAChR-binding proteins like  $\alpha$ -bungarotoxin (Tsetlin, 2014) and *LYNX1* (Lyukmanova et al., 2013).

To examine the possible effect of the mutation at the molecular level, we performed computational modeling and simulations of *LYNX2* binding to the  $\alpha 7$ : $\alpha 7$  interfaces of  $\alpha 7$  nAChR (Figure 2), a common nAChR subtype expressed in anxiety pathways of rodents

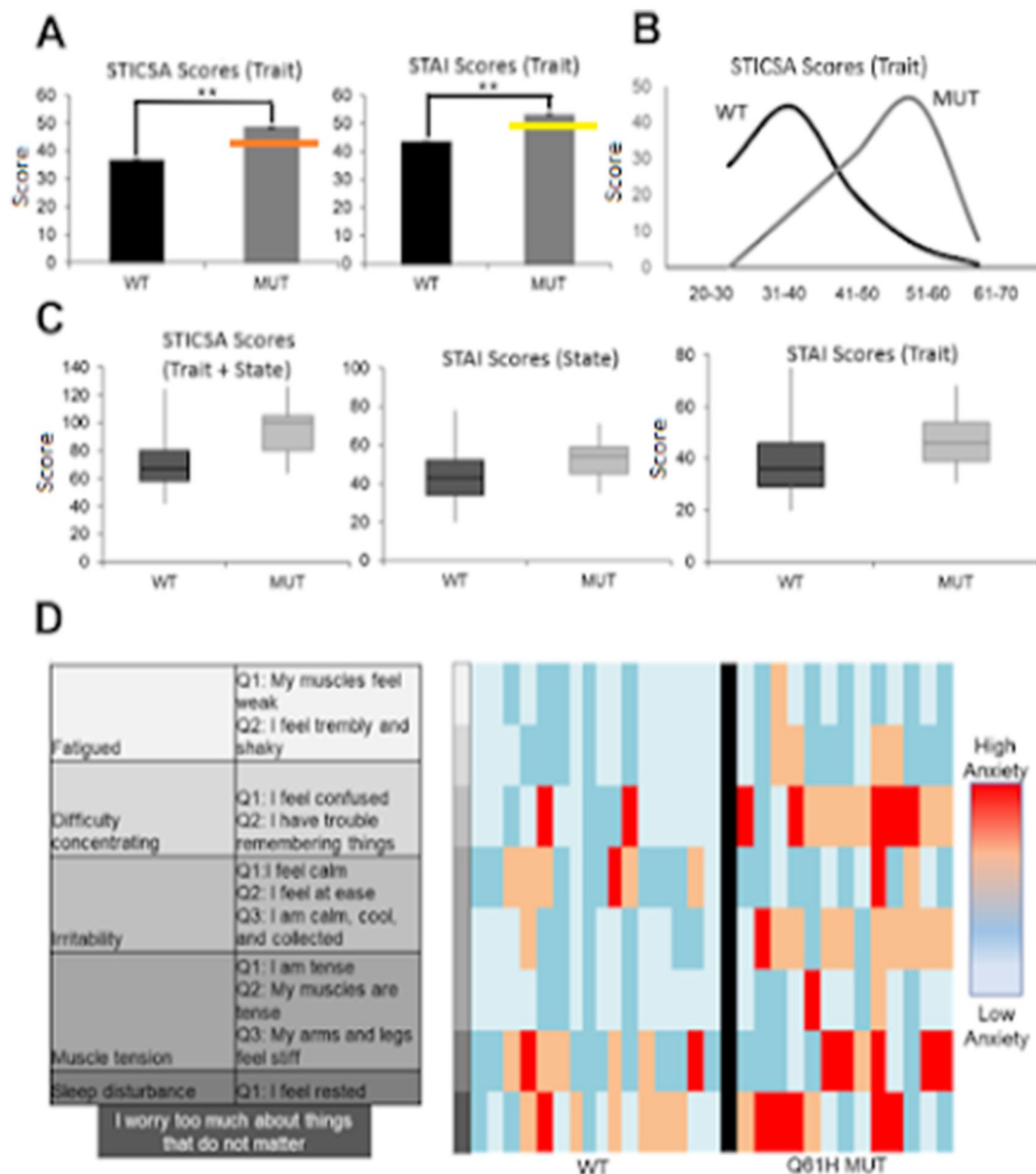


FIGURE 3

Individuals harboring *LYNX2* mutations have increased anxiety levels. **(A)** Wildtype (WT) and mutant (MUT) anxiety scores, STICSA trait (left) and STAI trait (right). Orange line is the level used to diagnose generalized anxiety disorder and the yellow line are scores at the level used to diagnose panic disorder population (STICSA:  $p < 1.0 \times 10^{-4}$ ,  $n = 558$  WT; 14 MUT; STAI:  $p = 4.0 \times 10^{-4}$ ,  $n = 553$  WT; 14 MUT Error bars represent  $\pm$ SEM). **(B)** Population histogram of STICSA trait, scores binned in 10 point increments. **(C)** Population box plot comparisons for STICSA total score (left), STAI state (middle), STAI trait (right). **(D)** DSM GAD criteria and corresponding questions from surveys (left), Monte Carlo WT and Q39H question responses (right). In the case of sleep disturbance, "I feel rested," low scores indicated disturbance and thus were converted to the same continuum.

and shown to be critical in regulating amygdala excitability (Klein and Yakel, 2006; Pidoplichko et al., 2013; Almeida-Suhett et al., 2014; Jiang et al., 2016). We chose the  $\alpha 7$  subtype to model because a homomeric subtype was more tractable to model than heteromeric nAChRs  $\alpha 4\beta 2$  and  $\alpha 4\beta 2$  subtypes. A low-resolution structural model of the  $\alpha 7$  nAChR in complex with *LYNX2* was generated based on our *LYNX1*/ $\alpha 4$ : $\alpha 4$  complex model (Nissen et al., 2018). A set of *LYNX2*/ $\alpha 7$ : $\alpha 7$  complex models was built by mapping each  $\alpha 7$  subunit (in the ensemble of 350  $\alpha 7$ : $\alpha 7$  conformations) and each *LYNX2* (in the ensemble of 50 *LYNX2* conformations) onto  $\alpha 4$ : $\alpha 4$  and *LYNX1* in the *LYNX1*/ $\alpha 4$ : $\alpha 4$  model, respectively, thus generating  $350 \times 50$

combinations. From this we selected the complex structure with the minimal number of energetically unfavorable contacts as the final model (Supplementary Figure S1).

The modeling indicates that the wild-type *LYNX2* forms a complex with the  $\alpha 7$ : $\alpha 7$  subunit interface through multiple salt bridges with E8, R46 and K70 of *LYNX2* (Figure 2B). However, in the Q39H *LYNX2* variant, the *LYNX2* and  $\alpha 7$ : $\alpha 7$  subunit interface salt bridges are established only by R46 of *LYNX2* (Figure 2B). Further, three residues in the loop II of WT *LYNX2*, including Q39, form additional hydrogen bonds with  $\alpha 7$ : $\alpha 7$ . These hydrogen bonds are, however, not observed in the  $\alpha 7$ : $\alpha 7$  complex with the Q39H variant *LYNX2*.

TABLE 2 Representative mutations found in this population along with anxiety scores.

GRCh37/hg19	Amino acid	Number of participants	STICSA	STICSA	STAI	STAI
Nucleotide position	Consequence	Found in study	State	Trait	State	Trait
WT	-	-	33.9	36.6	37.9	43.2
133426094	I23M	1	37	48	34	54
133426070	F31F	2	33, 37	44, 33	37, 38	44, 32
133426058	N35N	1	34	43	42	53
133426040	E41E	1	33	26	34	51
133426034	I43I	2	37, 29	38, 33	41, 40	43, 41
133426019	V48V	1	36	36	42	50
133425980	Q61H	14	45.9	48.4	46.9	54.0
133425984	E60V	2	28, -	33, -	33, -	35, -
13340373	Frameshift	1	51	68	45	53

Amino acid positions reference the full length protein. Note that some of the mutations are synonymous mutations and do not change the amino acid identity at that position.

TABLE 3 Cohort information.

		Discovery Cohort			Replication Cohort		
Total (n)		140			484		
Gender		56 M/84 F			12 M/332 F		
	WT	Mut	WT vs. MUT	WT	Mut	WT vs. MUT	
n	131	9		469	15		
Mutant info		5-Q61H			9-Q61H		
		1-V48V			1-E60V		
		1-E41E			2-I43I		
		2-F31F			1-N35N		
					1-I23M		
					1-Frameshift		
STICSA Total Score +/- SEM*	68.69 +/- 1.36	95.8 +/- 8.01	<i>p</i> = 0.013; Cohen's <i>d</i> = 1.64	71.09 +/- 1.04	91.778 +/- 6.184	<i>p</i> = 0.005; Cohen's <i>d</i> = 1.34	
STAI Total Score +/- SEM*	76.85 +/- 1.59	101.6 +/- 9.18	<i>p</i> = 0.026; Cohen's <i>d</i> = 1.31	82.76 +/- 1.30	99.0 +/- 6.53	<i>p</i> = 0.019; Cohen's <i>d</i> = 0.82	

General information and human anxiety test scores from a discovery and replication cohort. Scores represent the combined "at the moment" and general test scores, and were analyzed by *t*-test. Amino acid positions reference the full-length protein.

We measured intermolecular interaction energy between  $\alpha 7:\alpha 7$  and LYNX2 during the 400 ns molecular dynamics (MD) simulations (Figure 2C). The results indicate a more favorable interaction of WT LYNX2 with  $\alpha 7:\alpha 7$  after 200 ns than the Q39H variant. Therefore, our modeling and simulations suggest that the Q39H LYNX2 variant would have a lower binding affinity to  $\alpha 7$ -nAChRs and thus suppresses the function of  $\alpha 7$ -nAChRs less than a WT protein.

To further gain insight into the molecular consequences of naturally occurring variants underlying the LYNX2/nAChR interactions, we applied single-molecule atomic force spectroscopy (AFM) to study the reaction kinetics between LYNX2 and  $\alpha 7$  nAChRs at the single-molecule level. For these studies, purified recombinant LYNX2 was covalently attached to an AFM cantilever and a SH-EP1 mammalian cell line stably expressing concatemeric  $\alpha 7$  nAChRs (Pisapati et al., 2021) were used (Figure 6A). LYNX2/ $\alpha 7$  nAChR interactions were analyzed by dynamic force spectroscopy (DFS), the plot of most probable unbinding force (Figure 6B, Equations 1–3). The

unbinding force of the LYNX2/ $\alpha 7$  nAChR interaction increased with the logarithm of the loading rate, ranging from 60 to 90 pN over a loading rate of 30–4,000 pN/s, respectively (Figure 6B, Equations 1–3). The LYNX2 variant with the Q39H mutation found in the human population resulted in significantly decreased unbinding force under all tested loading rates tested. The mutation shortened the lifetime of the interaction by 180-fold (from 1,470 to 8.1 s). This result indicates that this human mutation in LYNX2 weakens the physical association with  $\alpha 7$  nAChRs *in vitro*.

## 4 Discussion

In this study, we have identified a correlation between the genomic presence of a LYNX2 variant, Q39H, and clinically relevant levels of anxiety in humans. The LYNX2 mutation we found in our population confers reduced binding affinity of the LYNX2 protein to its target,

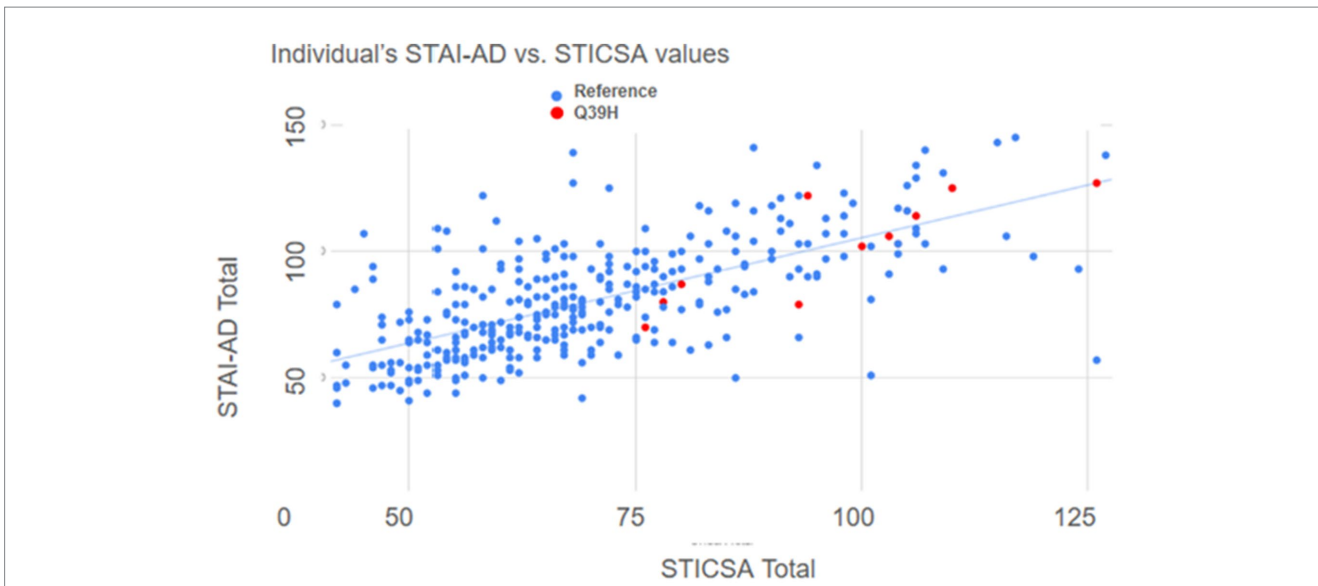


**FIGURE 4**  
Correlation between STICSA and STAI values by individual. Scatter plot of anxiety scores; STICSA values combining both “at the moment” plus general values of that test, on the x-axis, plotted against the combined STAI values, “at the moment” plus general values, on the y axis. Each dot represents a different individual. Blue represents individuals with the WT *LYNX2* gene and red represents those harboring the Q39H *LYNX2* mutation.

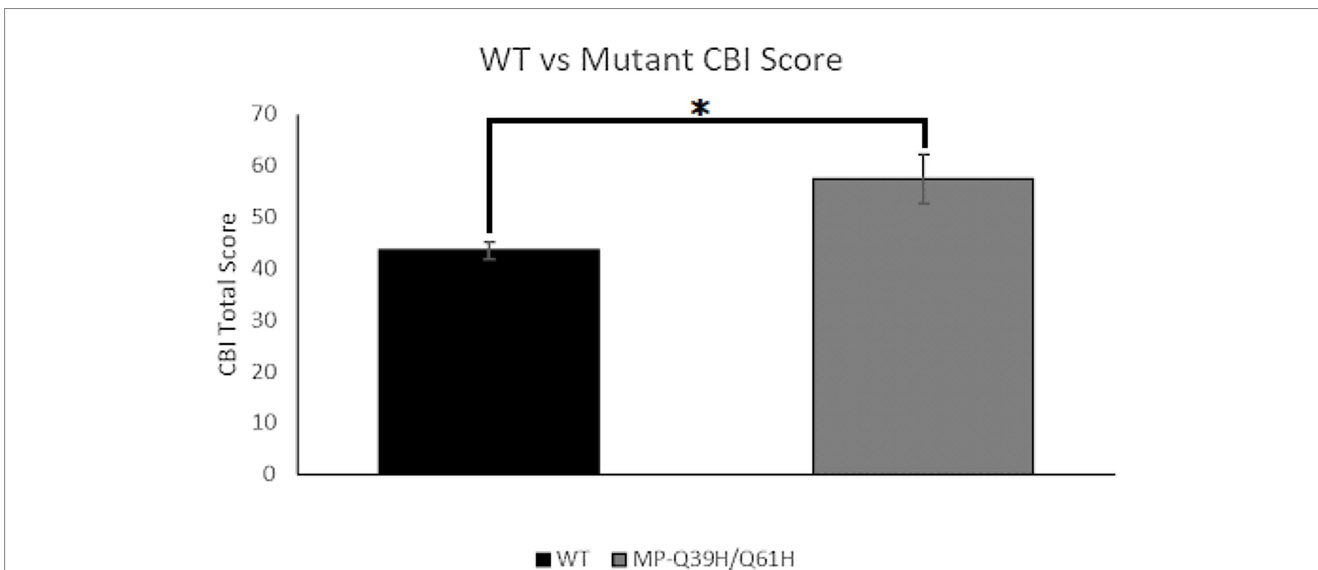
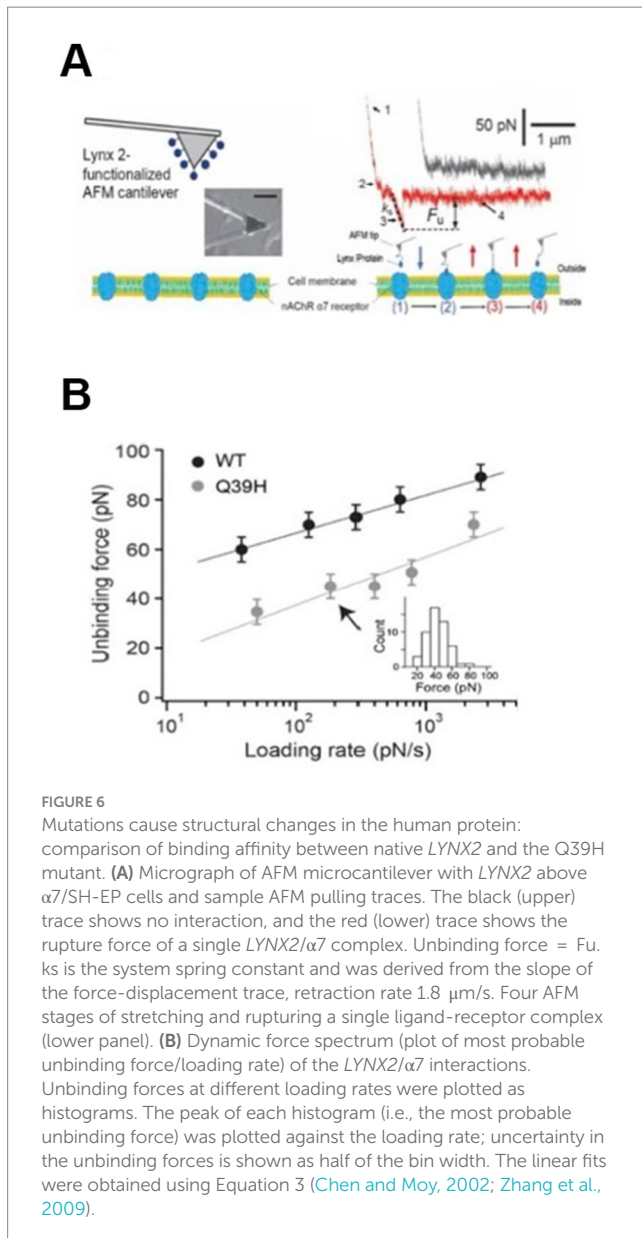


**FIGURE 5**  
Creative behavioral inventory (CBI) score comparison. Average CBI score for wildtype (WT) vs. Q39H ( $n = 206$  WT;  $n = 9$  Q39H). Data were analyzed using a Fisher Exact Test with a threshold CBI score of 40, in which data were organized into a category of a score either  $<40$  or  $\geq 40$  ( $p = 0.0447$ ).

nAChRs. Taken together, reduced binding of the *LYNX2* protein that results from the Q39H mutation, in some cases, could result in abnormal anxiety levels in individuals harboring the mutation.

We found that the most common human *LYNX2* variant, Q39H, was associated with responses that aligned with the DSM criteria for anxiety disorder diagnoses, GAD and panic disorder. The behavioral expression of fear results from a relative weighting of key components of the circuits underlying fear behavior. Murine *Lynx2* is expressed in several of these key regions in mice, including the prefrontal cortex and amygdala (Tekinay et al., 2009; Dessaud et al., 2006). The amygdala is an important structure in basal fear and anxiety behavior in humans (Martin et al., 2009; LeDoux, 2011), whereas the prefrontal

cortex can have roles in assessing and modifying fear-based learning association (Fanselow and LeDoux, 1999; Sierra-Mercado et al., 2010; Ottaviani et al., 2012; Lebois et al., 2019; Morgan et al., 1993; Milad and Quirk, 2002; Quirk et al., 2000; Milad et al., 2006; Sierra-Mercado et al., 2010; Amano et al., 2010; Do-Monte et al., 2015; Mukherjee et al., 2018). Any factor which alters the normal activity in these circuits (amygdala, prefrontal cortex and limbic cortex) may influence anxiety levels. nAChRs have been implicated in the regulation of anxiety (Mineur et al., 2023). A mutation in a nAChR modulator such as *LYNX2*, that disrupts the normal binding capability, protein levels, or activity has the potential to play a role in the regulation of anxiety by altering nAChR function.



The Q39H mutation led to a *LYNX2* variant with decreased binding affinity to  $\alpha 7$  nAChRs, which to our knowledge, is the first demonstration of a naturally occurring mutation in the human *LYNX2* protein with a defined biological or biophysical consequence (Anderson et al., 2020). Furthermore, the binding data provide compelling evidence that the human *LYNX2* gene operates in a similar manner as mouse *Lynx2* via its modulation of nAChRs. In *Lynx2* null mutant mice, nAChR responses are hyperactive, responding with hypersensitivity to agonist and slower desensitization rates. This perturbation is accompanied by elevations in both basal and state anxiety-like behavior (Tekinay et al., 2009). In the case of the human Q39H carriers, we suggest that *LYNX2* protein is expressed but does not have the binding, and in turn inhibitory capability, of wild-type *LYNX2*, the consequence of which is nAChR hypersensitivity and elevated anxiety levels.

Although the heightened anxiety scores seen in the variant/alternate allele subpopulations match those of diagnosed population levels, our population does not report a high percentage of clinical

diagnosis, likely due to the age of participants in our study ( $M = 20$  years of age). Although the predicted age of onset of anxiety disorders was found to average 21.3 years of age in a meta-analysis, anxiety disorders at the time of this study were often not clinically diagnosed until 30 years of age (Gonçalves and Byrne, 2012; Vaingankar et al., 2013; Lijster et al., 2017). In addition, median age of onset varies greatly depending on the disorder; while the GAD median age of onset is 30, social anxiety and specific phobia diagnosis typically occur earlier in life, most often during adolescence. The majority of our cohort being students, they face a composite of stressors different from that of older populations. As such, it cannot be predicted if a similar incidence would be found in older individuals. Because of the select nature of the cohort tested, investigation of this variant in the general population including a greater number of older individuals would be helpful in evaluating the persistence of the effect of such a mutation on anxiety levels. Not all the carriers in our cohort exhibited higher than normal levels of anxiety (>60% of Q39H carriers exhibited elevated anxiety levels, compared to <20% in the reference group), underscoring the complex nature of anxiety and as would be expected, other factors than a single gene would play into the behavioral expression of anxiety (Parodi et al., 2022). The Q39H allele is novel and not found in databases, so caution must be applied to the interpretation of these findings. A new mutation at the same nucleotide position was entered into a human database subsequent to the time period of data collection indicating that novel mutations in the *LYNX2* gene may still be forthcoming.

It would be interesting to test if the Q39H mutation occurred at a higher rate in the GAD or panic disorder population as compared to a general population. Identifying individuals with susceptibility toward anxiety in such a way could enable earlier preventative measures, such as monitoring, stress management techniques or psychotherapy. This would be significant as unregulated anxiety can lead, not only to an anxiety disorder, but also to depression (Maron and Nutt, 2017). There is potential for *LYNX2* to have utility as a genetic screen to aid in identification of susceptible individuals before anxiety becomes severe or an entrenched disorder. Such a genetic screen could be an advance given the paucity of biomarkers for mental illnesses. Recently, there have been reports that expression differences of *LYNX2* may help to differentiate Bipolar Disorder from Schizophrenia and MDD (Shen et al., 2024). Natural variation in the *Lynx2* gene, however, has been associated only in animal strains that exhibit altered fear conditioning (Parker et al., 2012), or with processes outside of the nervous system, such as cancer and skin abnormalities (Sugimori et al., 2024; Song et al., 2024).

Though we tested binding of the *LYNX2* protein to  $\alpha 7$  nAChRs by AFM, we did not test for binding of other known targets of *LYNX2*, such as  $\alpha 3\beta 4$  and  $\alpha 4\beta 2$  subtypes, and it would be worthwhile to investigate binding of Q39H protein on those subtypes as well. It is worth noting the potential relevance of *LYNX2*'s interaction with  $\alpha 3\beta 4$  nAChRs, a subtype that has been implicated in anxiety regulation in brain regions such as the medial habenula and the interpeduncular nucleus (IPN) (McLaughlin et al., 2017; Molas et al., 2017). *LYNX2* has been found to bind with higher affinity to  $\alpha 3\beta 4$  nAChRs as compared to  $\alpha 7$  nAChRs (Pisapati et al., 2021), and thus  $\alpha 3\beta 4$  nAChRs are a probable target of the effect of *LYNX2* action. The medial habenula/IPN has been implicated mediating anxiety induced by nicotine withdrawal (Molas et al., 2017), and is a region that highly expresses  $\alpha 3$  and  $\beta 4$  nAChR subunits (Grady et al., 2009). The cohort examined in this study contained a low level of those self-reporting

nicotine intake. Further studies on a smoking population or those subject to nicotine dependence may bring insights into the effect of human *LYNX2* and  $\alpha 3\beta 4$  nAChRs. In-depth studies on  $\alpha 3\beta 4$  might be fruitful by performing nicotine withdrawal tests in the *Lynx2* KO mouse model and focusing on the medial habenula/IPN pathway. The  $\alpha 7$  nAChR subtype has been shown to play a role in anxiety-like regulation of animal behavior (O'Connor et al., 2024; Mineur et al., 2023). Further, *CHRNA7*, the gene that encodes  $\alpha 7$  nAChRs, has been associated with anxiety and depressive disorders in clinical trials (Gillentine et al., 2018). Polymorphisms in the human *CHRNA4* gene, which encodes the  $\alpha 4$  nAChR subunit, has been linked to anxiety and emotional lability (Markett et al., 2011), and  $\alpha 4\beta 2$  nAChRs have been linked to anxiety in a number of studies (McGranahan et al., 2011; Mineur et al., 2023). The nAChR target of *LYNX2* has been reported for  $\alpha 4\beta 2$ ,  $\alpha 7$ , and  $\alpha 3\beta 4$  nAChR, but the interaction of *LYNX2* on other subtypes, such as  $\alpha 4\beta 4$ ,  $\alpha 6$ - or  $\alpha 5$ -containing nAChRs, etc. to our knowledge has not been tested as yet. Much further work will be necessary to understand the binding of *LYNX2* on different nAChR subtypes and their effects on different CNS processes.

*LYNX2* expression is not confined to the anxiety-related circuit, and thus some of the elevated anxiety phenotype could be amplified or blunted by effects from other regions or influence other processes that were not measured here. Another potential explanation for the lower percentage of carriers exhibiting low levels of anxiety diagnoses, could be rooted in the fact that this variant/alternate allele subpopulation also displays heightened scores used to measure human creativity, indicating a potential, previously suggested, association between creativity and anxiety (Kyaga et al., 2012). Studies show that creative outlets may be used to temporarily decrease anxiety supporting this potential correlation (Müller et al., 2008; King et al., 2013). Further, human studies have shown a relationship between enhanced associative learning and creative thought (Beaty and Kenett, 2023). While not directly translatable, *Lynx2* KO mice demonstrate elevated associative learning in a fear-conditioning paradigm (Tekinay et al., 2009). Since these mice also demonstrate elevated basal levels of anxiety-like behavior, this phenotype cannot be directly interpreted as enhanced learning. This mouse model does, however, demonstrate heightened responses to a nAChR agonist in the prefrontal cortex, measured by EPSC rate, suggesting a physiological consequence and possible alterations in circuit function (Tekinay et al., 2009) and behaviors (Sherafat et al., 2021) outside the amygdala. Further characterization of the allele in humans has the potential to shed light on the neural processes enabling novel or creative thought and/or provide a biological explanation for the correlation between creative individuals and mental illness (Andreasen, 1987; Runco and Richards, 1997; Kyaga et al., 2011; Kyaga et al., 2012).

Our data suggest a potential diagnostic avenue for those suffering from an anxiety disorder by identifying individuals harboring a deleterious *LYNX2* mutation that may sensitize nAChRs within specific neural circuits. Despite compelling evidence of the role of nAChRs in affective disorders, large clinical trials targeting nAChRs have failed, demonstrating that targeting of nAChRs in a general population is not generally effective (Vieta et al., 2013). Smaller studies with specific inclusion criteria have shown success clinically (Phillips et al., 2005), raising the possibility that nAChR targeting could be a more effective treatment within a specific subpopulation. Genetic discriminators may be one such defining marker. A genetically identified subpopulation harboring this *LYNX2* mutation, entered into clinical trials may lead to better outcomes for nAChR candidates than when tested in a general population of individuals with better

moderated nAChR responses. Alternatively, it may identify those who may be responsive to already approved medications such as the nAChR blocker mecamylamine (Bacher et al., 2009). These results have implications for the much-needed early identification of those with a genetic predisposition to anxiety, and hence for the possible prevention of the development of an anxiety disorder.

## Data availability statement

The original contributions presented in the study are included in the article/Supplementary materials, further inquiries can be directed to the corresponding author.

## Ethics statement

The studies involving humans were approved by Institutional Review Board (IRB). The studies were conducted in accordance with the local legislation and institutional requirements. The participants provided their written informed consent to participate in this study. The animal study was approved by institutional animal care and use committee (IACUC). The study was conducted in accordance with the local legislation and institutional requirements.

## Author contributions

KA: Writing – review & editing, Writing – original draft, Visualization, Validation, Methodology, Formal analysis, Data curation, Conceptualization. WC: Conceptualization, Data curation, Formal analysis, Methodology, Writing – review & editing. HL: Formal analysis, Validation, Writing – original draft. MC: Writing – review & editing, Writing – original draft. TP: Formal analysis, Validation, Writing – review & editing, Writing – original draft. EF-P: Formal analysis, Validation, Writing – original draft, Writing – review & editing. AD: Writing – original draft. PR: Writing – original draft. MB: Writing – review & editing, Writing – original draft. GG: Writing – original draft, Writing – review & editing. AP: Writing – original draft. KH: Writing – original draft, Writing – review & editing, Data curation, Methodology, Validation, Supervision. KM: Conceptualization, Data Curation, Supervision, Writing – review & editing. AH: Writing – review & editing, Writing – original draft. WI: Conceptualization, Methodology, Supervision, Funding acquisition, Writing – review & editing, Writing – original draft. XZ: Conceptualization, Methodology, Supervision, Formal Analysis, Funding acquisition, Writing – original draft, Writing – review & editing. JM: Writing – review & editing, Visualization, Validation, Supervision, Resources, Project administration, Methodology, Investigation, Funding acquisition, Formal analysis, Data curation, Conceptualization, Writing – original draft.

## Funding

The author(s) declare that financial support was received for the research, authorship, and/or publication of this article. This work was supported by NSF 1745823, R01GM123131, 5R01DA043567, NIH R01 GM126140, R44 DA032464, and R21DA033831, XSEDE MCB070009, Danish Research Foundation/Det Frie Forskningsråd,

Lehigh Accelerate, PA CURE 4100068719, Lehigh University College of Arts and Sciences Graduate Student Grant, Sigma Xi GAIR.

## Acknowledgments

The authors wish to thank Marina Picciotto for critical reading of the manuscript, Paul Whiteaker for the gift of the  $\alpha 7$  cell line, Khanjan Mehta, Bill Whitney, Nancy Wayne, Meg Kenna, Murray Itzkowitz, David Cundall, Kyra L. Feuer, Samantha Eichelberger, Ben Davis, Trishna Dave, Maggie Dalena, Neel Nissen, Jen Golley, Sana Ali, Reem Azar, Chris Hoke, Andy Truman, Mountaintop, BSDI, RARE, BioConnect, Teagle Foundation, CINQ, BioS279 groups for technical and/or project support and the Biological Sciences Department.

## Conflict of interest

The authors declare that the research was conducted in the absence of any commercial or financial relationships that could be construed as a potential conflict of interest.

## References

- Almeida-Suhett, C. P., Prager, E. M., Pidoplichko, V., Figueiredo, T. H., Marini, A. M., Li, Z., et al. (2014). Reduced GABAergic inhibition in the basolateral amygdala and the development of anxiety-like behaviors after mild traumatic brain injury. *PLoS One* 9:e102627. doi: 10.1371/journal.pone.0102627
- Amano, T., Unal, C. T., and Pare, D. (2010). Synaptic correlates of fear extinction in the amygdala. *Nat. Neurosci.* 13, 489–494. doi: 10.1038/nn.2499
- Anderson, K. R., Hoffman, K. M., and Miwa, J. M. (2020). Modulation of cholinergic activity through lynx prototoxins: implications for cognition and anxiety regulation. *Neuropharmacology* 174:108071. doi: 10.1016/j.neuropharm.2020.108071
- Andreasen, N. C. (1987). Creativity and mental illness: prevalence rates in writers and their first-degree relatives. *Am. J. Psychiatry* 144, 1288–1292. doi: 10.1176/ajp.144.10.1288
- Bacher, I., Wu, B., Shytle, D. R., and George, T. P. (2009). Mecamylamine – a nicotinic acetylcholine receptor antagonist with potential for the treatment of neuropsychiatric disorders. *Expert. Opin. Pharmacother.* 10, 2709–2721. doi: 10.1517/14656560903329102
- Bandelow, B., and Michaelis, S. (2015). Epidemiology of anxiety disorders in the 21st century. *Dialogues Clin. Neurosci.* 17, 327–335. doi: 10.31887/DCNS.2015.17.3/bandelow
- Beaty, R. E., and Kenett, Y. N. (2023). Associative thinking at the core of creativity. *Trends Cogn. Sci.* 27, 671–683. doi: 10.1016/j.tics.2023.04.004
- Bell, G. I. (1978). Models for the specific adhesion of cells to cells. *Science* 200, 618–627. doi: 10.1126/science.347575
- Bystritsky, A., Khalsa, S. S., Cameron, M. E., and Schiffman, J. (2013). Current diagnosis and treatment of anxiety disorders. *Pharm. Ther.* 38, 30–57.
- Chambers, J. A., Power, K. G., and Durham, R. C. (2004). The relationship between trait vulnerability and anxiety and depressive diagnoses at long-term follow-up of generalized anxiety disorder. *J. Anxiety Disord.* 18, 587–607. doi: 10.1016/j.janxdis.2003.09.001
- Chen, A., and Moy, V. T. (2002). Single-molecule force measurements. *Methods Cell Biol.* 68, 301–309. doi: 10.1016/s0091-679x(02)68015-x
- Dessaud, E., Salaün, D., Gayet, O., Chabbert, M., and deLapeyrière, O. (2006). Identification of lynx2, a novel member of the ly-6/neurotoxin superfamily, expressed in neuronal subpopulations during mouse development. *Mol. Cell. Neurosci.* 31, 232–242. doi: 10.1016/j.mcn.2005.09.010
- Do-Monte, F. H., Manzano-Nieves, G., Quiñones-Laracuente, K., Ramos-Medina, L., and Quirk, G. J. (2015). Revisiting the Role of Infralimbic cortex in fear extinction with Optogenetics. *J. Neurosci.* 35, 3607–3615. doi: 10.1523/JNEUROSCI.3137-14.2015
- Dong, C., Kern, N. R., Anderson, K. R., Zhang, X. E., Miwa, J. M., and Im, W. (2020). Dynamics and interactions of GPI-linked lynx1 protein with/without nicotinic acetylcholine receptor in membrane bilayers. *J. Phys. Chem. B* 124, 4017–4025. doi: 10.1021/acs.jpcc.0c00159
- Duits, P., Cath, D. C., Lissek, S., Hox, J. J., Hamm, A. O., Engelhard, I. M., et al. (2015). Updated meta-analysis of classical fear conditioning in anxiety disorders. *Depress. Anxiety* 32, 239–253. doi: 10.1002/da.22353
- Ebner, A., Wildling, L., Kamruzzahan, A. S., Rankl, C., Wruss, J., Hahn, C. D., et al. (2007). A new, simple method for linking of antibodies to atomic force microscopy tips. *Bioconjug. Chem.* 18, 1176–1184. doi: 10.1021/bc070030s
- Elwood, L. S., Wolitzky-Taylor, K., and Olatunji, B. O. (2012). Measurement of anxious traits: a contemporary review and synthesis. *Anxiety Stress Coping* 25, 647–666. doi: 10.1080/10615806.2011.582949
- Evans, E. (2001). Probing the relation between force–lifetime–and chemistry in single molecular bonds. *Annu. Rev. Biophys. Biomol. Struct.* 30, 105–128. doi: 10.1146/annurev.biophys.30.1.105
- Evans, E., and Ritchie, K. (1997). Dynamic strength of molecular adhesion bonds. *Biophys. J.* 72, 1541–1555. doi: 10.1016/S0006-3495(97)78802-7
- Fanselow, M. S., and LeDoux, J. E. (1999). Why we think plasticity underlying Pavlovian fear conditioning occurs in the basolateral amygdala. *Neuron* 23, 229–232. doi: 10.1016/s0896-6273(00)80775-8
- Feder, A., Nestler, E. J., and Charney, D. S. (2009). Psychobiology and molecular genetics of resilience. *Nat. Rev. Neurosci.* 10, 446–457. doi: 10.1038/nrn2649
- Fu, X., Xu, Y., Wu, C., Moy, V. T., and Zhang, X. (2015). Anchorage-dependent binding of integrin I-domain to adhesion ligands. *J. Mol. Recognit.* 28, 385–392. doi: 10.1002/jmr.2453
- Gillentine, M., Lozoya, R., Yin, J., Grochowski, C., White, J., Schaaf, C., et al. (2018). a7 nAChRs have been linked to anxiety and depression, and CHRNA7 copy number gains have been found enriched in adolescents with major depressive and anxiety disorders. *J. Affect. Disord.* 239, 247–252. doi: 10.1016/j.jad.2018.07.017
- Gonçalves, D. C., and Byrne, G. J. (2012). Interventions for generalized anxiety disorder in older adults: systematic review and meta-analysis. *J. Anxiety Disord.* 26, 1–11. doi: 10.1016/j.janxdis.2011.08.010
- Grady, S. R., Moretti, M., Zoli, M., Marks, M. J., Zanardi, A., Pucci, L., et al. (2009). Rodent habenulo-interpeduncular pathway expresses a large variety of uncommon nAChR subtypes, but only the alpha3beta4\* and alpha3beta3beta4\* subtypes mediate acetylcholine release. *J. Neurosci.* 29, 2272–2282. doi: 10.1523/JNEUROSCI.5121-08.2009
- Gröbs, D. F., Antony, M. M., Simms, L. J., and McCabe, R. E. (2007). Psychometric properties of the state-trait inventory for cognitive and somatic anxiety (STICSA): comparison to the state-trait anxiety inventory (STAI). *Psychol. Assess.* 19, 369–381. doi: 10.1037/1040-3590.19.4.369
- Hascoët, M., Bourin, M., and Nic Dhonnchadha, B. A. (2001). The mouse light-dark paradigm: a review. *Prog. Neuro-Psychopharmacol. Biol. Psychiatry* 25, 141–166. doi: 10.1016/s0278-5846(00)00151-2
- Huang, J., Rauscher, S., Nawrocki, G., Ran, T., Feig, M., de Groot, B. L., et al. (2017). CHARMM36m: an improved force field for folded and intrinsically disordered proteins. *Nat. Methods* 14, 71–73. doi: 10.1038/nmeth.4067

## Generative AI statement

The authors declare that no Generative AI was used in the creation of this manuscript.

## Publisher's note

All claims expressed in this article are solely those of the authors and do not necessarily represent those of their affiliated organizations, or those of the publisher, the editors and the reviewers. Any product that may be evaluated in this article, or claim that may be made by its manufacturer, is not guaranteed or endorsed by the publisher.

## Supplementary material

The Supplementary material for this article can be found online at: <https://www.frontiersin.org/articles/10.3389/fnbeh.2024.1347543/full#supplementary-material>

- Hutter, J. L., and Bechhoefer, J. (1993). Calibration of atomic-force microscope tips. *Rev. Sci. Instrum.* 64, 1868–1873. doi: 10.1063/1.1143970
- Jiang, L., Kundu, S., Lederman, J. D., López-Hernández, G. Y., Ballinger, E. C., Wang, S., et al. (2016). Cholinergic signaling controls conditioned fear behaviors and enhances plasticity of cortical-amygdala circuits. *Neuron* 90, 1057–1070. doi: 10.1016/j.neuron.2016.04.028
- Jo, S., Kim, T., Iyer, V. G., and Im, W. (2008). CHARMM-GUI: a web-based graphical user interface for CHARMM. *J. Comput. Chem.* 29, 1859–1865. doi: 10.1002/jcc.20945
- Kayikcioglu, O., Bilgin, S., Seymenoglu, G., and Devenci, A. (2017). State and trait anxiety scores of patients receiving Intravitreal injections. *Biomed. Hub* 2, 1–5. doi: 10.1159/000478993
- King, R., Neilsen, P., and White, E. (2013). Creative writing in recovery from severe mental illness. *Int. J. Ment. Health Nurs.* 22, 444–452. doi: 10.1111/j.1447-0349.2012.00891.x
- Klein, R. C., and Yakel, J. L. (2006). Functional somato-dendritic alpha7-containing nicotinic acetylcholine receptors in the rat basolateral amygdala complex. *J. Physiol.* 576, 865–872. doi: 10.1113/jphysiol.2006.118232
- Kyaga, S., Landén, M., Boman, M., Hultman, C. M., Långström, N., and Lichtenstein, P. (2012). Mental illness, suicide and creativity: 40-year prospective total population study. *J. Psychiatr. Res.* 47, 83–90. doi: 10.1016/j.jpsychires.2012.09.010
- Kyaga, S., Lichtenstein, P., Boman, M., Hultman, C., Långström, N., and Landén, M. (2011). Creativity and mental disorder: family study of 300,000 people with severe mental disorder. *Br. J. Psychiatry* 199, 373–379. doi: 10.1192/bjp.bp.110.085316
- Lebois, L., Seligowski, A. V., Wolff, J. D., Hill, S. B., and Ressler, K. J. (2019). Augmentation of extinction and inhibitory learning in anxiety and trauma-related disorders. *Annu. Rev. Clin. Psychol.* 15, 257–284. doi: 10.1146/annurev-clinpsy-050718-095634
- LeDoux, J. E. (2011). Emotion circuits in the brain. *Annu. Rev. Neurosci.* 23, 155–184. doi: 10.1146/annurev.neuro.23.1.155
- Lee, J., Cheng, X., Swails, J. M., Yeom, M. S., Eastman, P. K., Lemkul, J. A., et al. (2016). CHARMM-GUI input generator for NAMD, GROMACS, AMBER, OpenMM, and CHARMM/OpenMM simulations using the CHARMM36 additive force field. *J. Chem. Theory Comput.* 12, 405–413. doi: 10.1021/acs.jctc.5b00935
- Le-Niculescu, H., Balaraman, Y., Patel, S. D., Ayalew, M., Gupta, J., Kuczenski, R., et al. (2011). Convergent functional genomics of anxiety disorders: translational identification of genes, biomarkers, pathways and mechanisms. *Transl. Psychiatry* 1:e9. doi: 10.1038/tp.2011.9
- Li, S. X., Huang, S., Bren, N., Noridomi, K., Dellisanti, C. D., Sine, S. M., et al. (2011). Ligand-binding domain of an  $\alpha 7$ -nicotinic receptor chimera and its complex with agonist. *Nat. Neurosci.* 14, 1253–1259. doi: 10.1038/nn.2908
- Lijster, J. M., Dierckx, B., Utens, E. M., Verhulst, F. C., Zieldorff, C., Dieleman, G. C., et al. (2017). The age of onset of anxiety disorders. *Can. J. Psychiatry* 62, 237–246. doi: 10.1177/0706743716640757
- Lissek, S., Kaczurkin, A. N., Rabin, S., Geraci, M., Pine, D. S., and Grillon, C. (2014). Generalized anxiety disorder is associated with overgeneralization of classically conditioned-fear. *Biol. Psychiatry* 75, 909–915. doi: 10.1016/j.biopsych.2013.07.025
- Locke, A. B., Kirst, N., and Shultz, C. G. (2015). Diagnosis and management of generalized anxiety disorder and panic disorder in adults. *Am. Fam. Physician* 91, 617–624.
- Lyukmanova, E. N., Shenkarev, Z. O., Shulepko, M. A., Mineev, K. S., D'Hoedt, D., Kasheverov, I. E., et al. (2011). NMR structure and action on nicotinic acetylcholine receptors of water-soluble domain of human LYNX1. *J. Biol. Chem.* 286, 10618–10627. doi: 10.1074/jbc.M110.189100
- Lyukmanova, E. N., Shulepko, M. A., Buldakova, S. L., Kasheverov, I. E., Shenkarev, Z. O., Reshetnikov, R. V., et al. (2013). Water-soluble LYNX1 residues important for interaction with muscle-type and/or neuronal nicotinic receptors. *J. Biol. Chem.* 288, 15888–15899. doi: 10.1074/jbc.M112.436576
- Maghrabi, A. H. A., and McGuffin, L. J. (2017). ModFOLD6: an accurate web server for the global and local quality estimation of 3D models of proteins. *Nucleic Acids Res.* 45, W416–W421. doi: 10.1093/nar/gkx332
- Markett, S., Montag, C., and Reuter, M. (2011). The nicotinic acetylcholine receptor gene CHRNA4 is associated with negative emotionality. *Emotion* 11, 450–455. doi: 10.1037/a0021784
- Maron, E., and Nutt, D. (2017). Biological markers of generalized anxiety disorder. *Dialogues Clin. Neurosci.* 19, 147–158. doi: 10.31887/DCNS.2017.19.2/dnutt
- Martin, E. I., Ressler, K. J., Binder, E., and Nemeroff, C. B. (2009). The neurobiology of anxiety disorders: brain imaging, genetics, and psychoneuroendocrinology. *Psychiatr. Clin. North Am.* 32, 549–575. doi: 10.1016/j.psc.2009.05.004
- McGranahan, T. M., Patzlaff, N. E., Grady, S. R., Heinemann, S. F., and Booker, T. K. (2011).  $\alpha 2$  nicotinic acetylcholine receptors on dopaminergic neurons mediate nicotine reward and anxiety relief. *J. Neurosci.* 31, 10891–10902. doi: 10.1523/JNEUROSCI.0937-11.2011
- McLaughlin, I., Dani, J. A., and De Biasi, M. (2017). The medial habenula and interpeduncular nucleus circuitry is critical in addiction, anxiety, and mood regulation. *J. Neurochem.* 142, 130–143. doi: 10.1111/jnc.14008
- Milad, M. R., and Quirk, G. J. (2002). Neurons in the medial prefrontal cortex signal memory for fear extinction. *Nature* 420, 70–74. doi: 10.1038/nature01138
- Milad, M. R., Rauch, S. L., Pitman, R. K., and Quirk, G. J. (2006). Fear extinction in rats: implications for human brain imaging and anxiety disorders. *Biol. Psychol.* 73, 61–71. doi: 10.1016/j.biopsycho.2006.01.008
- Mineur, Y. S., Fote, G. M., Blakeman, S., Cahuzac, E. L., Newbold, S. A., and Picciotto, M. R. (2016). Multiple nicotinic acetylcholine receptor subtypes in the mouse amygdala regulate affective behaviors and response to social stress. *Neuropsychopharmacology* 41, 1579–1587. doi: 10.1038/npp.2015.316
- Mineur, Y. S., Soares, A. R., Etherington, I. M., Abdulla, Z. I., and Picciotto, M. R. (2023). Pathophysiology of nAChRs: limbic circuits and related disorders. *Pharmacol. Res.* 191:106745. doi: 10.1016/j.phrs.2023.106745
- Miwa, J. M., Anderson, K. R., and Hoffman, K. M. (2019). Lynx Prototoxins: roles of endogenous mammalian neurotoxin-like proteins in modulating nicotinic acetylcholine receptor function to influence complex biological processes. *Front. Pharmacol.* 10:343. doi: 10.3389/fphar.2019.00343
- Molas, S., DeGroot, S. R., Zhao-Shea, R., and Tapper, A. R. (2017). Anxiety and Nicotine Dependence: Emerging Role of the Habenulo-Interpeduncular Axis. *Trends Pharmacol. Sci.* 38, 169–180. doi: 10.1016/j.tips.2016.11.001
- Morgan, M. A., Romanski, L. M., and LeDoux, J. E. (1993). Extinction of emotional learning: contribution of medial prefrontal cortex. *Neurosci. Lett.* 163, 109–113. doi: 10.1016/0304-3940(93)90241-c
- Mouro Ferraz Lima, T., Castaldelli-Maia, J. M., Apter, G., and Leopoldo, K. (2023). Neurobiological associations between smoking and internalizing disorders. *Int. Rev. Psychiatry (Abingdon, England)*, 35, 486–495. doi: 10.1080/09540261.2023.2252907
- Moylan, S., Jacka, F. N., Pasco, J. A., and Berk, M. (2012). Cigarette smoking, nicotine dependence and anxiety disorders: a systematic review of population-based, epidemiological studies. *BMC Med.* 10:123. doi: 10.1186/1741-7015-10-123
- Mukherjee, S., Tucker-Burden, C., Kaissi, E., Newsam, A., Duggireddy, H., Chau, M., et al. (2018). CDK5 inhibition resolves PKA/cAMP-independent activation of CREB1 signaling in glioma stem cells. *Cell Rep.* 23, 1651–1664. doi: 10.1016/j.celrep.2018.04.016
- Müller, E., Schuler, A., and Yates, G. B. (2008). Social challenges and supports from the perspective of individuals with Asperger syndrome and other autism spectrum disabilities. *Autism* 12, 173–190. doi: 10.1177/1362361307086664
- Nissen, N. I., Anderson, K. R., Wang, H., Lee, H. S., Garrison, C., Eichelberger, S. A., et al. (2018). Augmenting the antinociceptive effects of nicotinic acetylcholine receptor activity through lynx1 modulation. *PLoS One* 13:e0199643. doi: 10.1371/journal.pone.0199643
- O'Leary, T. P., Gunn, R. K., and Brown, R. E. (2013). What are we measuring when we test strain differences in anxiety in mice? *Behav. Genet.* 43, 34–50. doi: 10.1007/s10519-012-9572-8
- O'Connor, S. M., Sleebs, B. E., Street, I. P., Flynn, B. L., Baell, J. B., Coles, C., et al. (2024). BNC210, a negative allosteric modulator of the alpha 7 nicotinic acetylcholine receptor, demonstrates anxiolytic- and antidepressant-like effects in rodents. *Neuropharmacology* 246:109836. doi: 10.1016/j.neuropharm.2024.109836
- Oei, T. P., Evans, L., and Crook, G. M. (1990). Utility and validity of the STAI with anxiety disorder patients. *Br. J. Clin. Psychol.* 29, 429–432. doi: 10.1111/j.2044-8260.1990.tb00906.x
- Ottaviani, C., Cevolani, D., Nucifora, V., Borlimi, R., Agati, R., Leonardi, M., et al. (2012). Amygdala responses to masked and low spatial frequency fearful faces: a preliminary fMRI study in panic disorder. *Psychiatry Res.* 203, 159–165. doi: 10.1016/j.psychres.2011.12.010
- Palumbo, T. B., and Miwa, J. M. (2023). Lynx1 and the family of endogenous mammalian neurotoxin-like proteins and their roles in modulating nAChR function. *Pharmacol. Res.* 194:106845. doi: 10.1016/j.phrs.2023.106845. PMID: 37437646
- Paramonov, A. S., Kocharovskaya, M. V., Tsarev, A. V., Kulbatskii, D. S., Loktyushov, E. V., Shulepko, M. A., et al. (2020). Structural diversity and dynamics of human three-finger proteins acting on nicotinic acetylcholine receptors. *Int. J. Mol. Sci.* 21:7280. doi: 10.3390/ijms21197280
- Parker, C. C., Sokoloff, G., Cheng, R., and Palmer, A. A. (2012). Genome-wide association for fear conditioning in an advanced intercross mouse line. *Behav. Genet.* 42, 437–448. doi: 10.1007/s10519-011-9524-8
- Parodi, K. B., Holt, M. K., Green, J. G., Porche, M. V., Koenig, B., and Xuan, Z. (2022). Time trends and disparities in anxiety among adolescents, 2012–2018. *Soc. Psychiatry Psychiatr. Epidemiol.* 57, 127–137. doi: 10.1007/s00127-021-02122-9
- Phillips, J. C., Braun, R., Wang, W., Gumbart, J., Tajkhorshid, E., Villa, E., et al. (2005). Scalable molecular dynamics with NAMD. *J. Comput. Chem.* 26, 1781–1802. doi: 10.1002/jcc.20289
- Picciotto, M. R. (2003). Nicotine as a modulator of behavior: beyond the inverted U. *Trends Pharmacol. Sci.* 24, 493–499. doi: 10.1016/S0165-6147(03)00230-X
- Pidoplichko, V., Prager, E. M., Aroniadou-Anderjaska, V., and Braga, M. F. (2013).  $\alpha 7$ -containing nicotinic acetylcholine receptors on interneurons of the basolateral amygdala and their role in the regulation of the network excitability. *J. Neurophysiol.* 110, 2358–2369. doi: 10.1152/jn.01030.2012

- Pisapati, A. V., Cao, W., Anderson, K. R., Jones, G., Holick, K. H., Whiteaker, P., et al. (2021). Biophysical characterization of lynx-nicotinic receptor interactions using atomic force microscopy. *FASEB Bioadv.* 3, 1034–1042. doi: 10.1096/fba.2021-00012
- Quirk, G. J., Russo, G. K., Barron, J. L., and Lebron, K. (2000). The role of ventromedial prefrontal cortex in the recovery of extinguished fear. *J. Neurosci.* 20, 6225–6231. doi: 10.1523/JNEUROSCI.20-16-06225.2000
- Ree, M. J., French, D., MacLeod, C., and Locke, V. (2008). Distinguishing cognitive and somatic dimensions of state and trait anxiety: development and validation of the state trait inventory for cognitive and somatic anxiety (STICSA). *Behav. Cogn. Psychother.* 36, 313–332. doi: 10.1017/S1352465808004232
- Runco, M. A., and Richards, R. (1997). Eminent creativity, everyday creativity, and health. Westport, CT: Greenwood Publishing.
- Salas, R., Pieri, F., Fung, B., Dani, J. A., and De Biasi, M. (2003). Altered anxiety-related responses in mutant mice lacking the beta4 subunit of the nicotinic receptor. *J. Neurosci.* 23, 6255–6263. doi: 10.1523/JNEUROSCI.23-15-06255.2003
- Shen, J., Xiao, C., Qiao, X., Zhu, Q., Yan, H., Pan, J., et al. (2024). A diagnostic model based on bioinformatics and machine learning to differentiate bipolar disorder from schizophrenia and major depressive disorder. *Schizophrenia (Heidelb)* 10:16. doi: 10.1038/s41537-023-00417-1
- Sherafat, Y., Chen, E., Lallai, V., Bautista, M., Fowler, J. P., Chen, Y. C., et al. (2021). Differential Expression Patterns of Lynx Proteins and Involvement of Lynx1 in Prepulse Inhibition. *Front. Behav. Neurosci.* 15:703748. doi: 10.3389/fnbeh.2021.703748
- Sierra-Mercado, D., Padilla-Coreano, N., and Quirk, G. J. (2010). Dissociable roles of prelimbic and infralimbic cortices, ventral hippocampus, and basolateral amygdala in the expression and extinction of conditioned fear. *Neuropsychopharmacology* 36, 529–538. doi: 10.1038/npp.2010.184
- Smelser, N. J., and Baltes, P. B. (2001). International encyclopedia of the social & behavioral sciences. New York City, NY: Elsevier Ltd., 560–567.
- Smith, C. A., and Kortemme, T. (2008). Backrub-like backbone simulation recapitulates natural protein conformational variability and improves mutant side-chain prediction. *J. Mol. Biol.* 380, 742–756. doi: 10.1016/j.jmb.2008.05.023
- Song, Z., Gui, S., Xiao, S., Rao, X., Cong, N., Deng, H., et al. (2024). A novel anoikis-related gene signature identifies LYPD1 as a novel therapy target for bladder cancer. *Sci. Rep.* 14:3198. doi: 10.1038/s41598-024-53272-0
- Spielberger, C. D., Gorsuch, R. L., Lushene, R., Vagg, P. R., and Jacobs, G. A. (1983). Manual for the state-trait anxiety inventory. Palo Alto, CA: Consulting Psychologists Press.
- Sugimori, A., Otori, I., Iwasawa, O., Saito, H., Nakajima, H., Matsuno, A., et al. (2024). Association of serum Ly6/PLAUR domain-containing protein 1 levels with skin sclerosis in systemic sclerosis. *Sci. Rep.* 14:5572. doi: 10.1038/s41598-024-56221-z
- Tekinay, A. B., Nong, Y., Miwa, J. M., Lieberam, I., Ibanez-Tallon, I., Greengard, P., et al. (2009). A role for LYNX2 in anxiety-related behavior. *Proc. Natl. Acad. Sci. USA* 106, 4477–4482. doi: 10.1073/pnas.0813109106
- Tsetlin, V. I. (2014). Three-finger snake neurotoxins and Ly6 proteins targeting nicotinic acetylcholine receptors: pharmacological tools and endogenous modulators. *Trends Pharmacol. Sci.* 36, 109–123. doi: 10.1016/j.tips.2014.11.003
- Vaigankar, J. A., Rekhi, G., Subramaniam, M., Abdin, E., and Chong, S. A. (2013). Age of onset of life-time mental disorders and treatment contact. *Soc. Psychiatry Psychiatr. Epidemiol.* 48, 835–843. doi: 10.1007/s00127-012-0601-y
- Van Dam, N. T., Gros, D. F., Earleywine, M., and Antony, M. M. (2013). Establishing a trait anxiety threshold that signals likelihood of anxiety disorders. *Anxiety Stress Coping* 26, 70–86. doi: 10.1080/10615806.2011.631525
- Vieta, E., Thase, M. E., Naber, D., D'Souza, B., Rancans, E., Lepola, U., et al. (2013). Efficacy and tolerability of flexibly-dosed adjunct TC-5214 (dexmecamylamine) in patients with major depressive disorder and inadequate response to prior antidepressant. *Eur. Neuropsychopharmacol.* 24, 564–574. doi: 10.1016/j.euroneuro.2013.12.008
- Wang, S., Zhu, X., Zhangsun, M., Wu, Y., Yu, J., Harvey, P. J., et al. Engineered Conotoxin Differentially Blocks and Discriminates Rat and Human  $\alpha 7$  Nicotinic Acetylcholine Receptors. *J. Med. Chem.* 64, 5620–5631. doi: 10.1021/acs.jmedchem.0c02079
- Wildling, L., Unterauer, B., Zhu, R., Rupprecht, A., Haselgrübler, T., Rankl, C., et al. (2011). Linking of sensor molecules with amino groups to amino-functionalized AFM tips. *Bioconjug. Chem.* 22, 1239–1248. doi: 10.1021/bc200099t
- Williams, T., Hattingh, C. J., Kariuki, C. M., Tromp, S. A., van Balkom, A. J., Ipser, J. C., et al. (2017). Pharmacotherapy for social anxiety disorder (SAnD). *Cochrane Database Syst. Rev.* 2019:CD001206. doi: 10.1002/14651858.CD001206.pub3
- Wilson, M. A., and Fadel, J. R. (2017). Cholinergic regulation of fear learning. *J. Neurosci. Res.* 95, 836–852. doi: 10.1002/jnr.23840
- Wu, M., Puddifoot, C. A., Taylor, P., and Joiner, W. J. (2015). Mechanisms of inhibition and potentiation of  $\alpha 4\beta 2$  nicotinic acetylcholine receptors by members of the Ly6 protein family. *J. Biol. Chem.* 290, 24509–24518. doi: 10.1074/jbc.M115.647248
- Yang, J., Yan, R., Roy, A., Xu, Y., Poisson, J., and Zhang, Y. (2015). The I-TASSER suite: protein structure and function prediction. *Nat. Methods* 12, 7–8. doi: 10.1038/nmeth.3213
- Zaigraev, M. M., Lyukmanova, E. N., Paramonov, A. S., Shenkarev, Z. O., and Chugunov, A. O. (2022). Orientational Preferences of GPI-Anchored Ly6/uPAR Proteins. *Int. J. Mol. Sci.* 24:11. doi: 10.3390/ijms24010011
- Zhao, L., Kuo, Y. P., George, A. A., Peng, J. H., Purandare, M. S., Schroeder, K. M., et al. (2003). Functional properties of homomeric, human alpha 7-nicotinic acetylcholine receptors heterologously expressed in the SH-EP1 human epithelial cell line. *J. Pharmacol. Exp. Ther.* 305, 1132–1141. doi: 10.1124/jpet.103.048777
- Zhang, X., Craig, S. E., Kirby, H., Humphries, M. J., and Moy, V. T. (2004). Molecular basis for the dynamic strength of the integrin alpha4beta1/VCAM-1 interaction. *Biophys. J.* 87, 3470–3478. doi: 10.1529/biophysj.104.045690
- Zhang, X., Rico, F., Xu, A. J., and Moy, V. T. (2009). "Atomic force microscopy of protein-protein interactions" in Handbook of single-molecule biophysics. eds. P. Hinterdorfer and A. Oijen (New York, NY: Springer).
- Zhang, X., Wojcikiewicz, E., and Moy, V. T. (2002). Force spectroscopy of the leukocyte function-associated antigen-1/intercellular adhesion molecule-1 interaction. *Biophys. J.* 83, 2270–2279. doi: 10.1016/S0006-3495(02)73987-8